

Research and Development Division
PORTLAND CEMENT ASSOCIATION
5420 Old Orchard Road
Skokie, Illinois

Literature Service Reports

(Informal reports prepared by the Literature Research and Library Group of the laboratory as a service to individual inquirers. Not for publication as Association releases.)

Class Foreign Literature Study

Date February 17, 1966

Serial No. 466

By Commercial Translator

For K. T. Burton
Structural Development Dept.

Translated from the Spanish: Diagonal Tension in Concrete Members of Circular Section

by Marco Jose Faradji Capon and
Roger Diaz de Cossio

Ingenieria, April 1965, pp. 257-280

Research and Development Division Library
Technical Information Department
Portland Cement Association
5420 Old Orchard Road
Skokie, Illinois

Diagonal Tension in Concrete Members of Circular Section

By Marco Jose Faradji Capon (*) and Roger Diaz de Cossio (**)

Ingenieria, April 1965, pp. 257-280

(Translated from the Spanish)

Foreign Literature Study No. 466

1. INTRODUCTION

1. Object

The object of this study was to obtain information on the shearing strength of reinforced concrete members of circular cross-section. This problem is not purely academic, for during the earthquakes of 1957 in Mexico City and of 1959 in Coatzacoalcos-Jaltipan numerous members of circular section were observed to have failed as a result of diagonal cracking.

When this research study began, the available literature did not contain sufficient information for designing circular sections for shear capacity.

Committee ACI-ASCE 426 (1) on shear and diagonal tension proposed an expression for calculating the shear capacity of rectangular members based on the results of about a thousand tests. The investigation reported in this paper was carried out making use of this information, and from the results obtained, an adaptation of the expression proposed by Committee 426 was made by redefining the parameters in order to evaluate the shear capacity of circular sections.

2. General description of the program

The test program consisted of 21 members, grouped in 15 types.

The members were tested in a horizontal position, and were loaded with either a single concentrated vertical load at midspan, or two concentrated loads placed near the third points.

(*) Research Scientist, Institute of Engineering and Prof. of the School of Engineering UNAM

(**) Research Scientist, Institute of Engineering; Chief of Doctorate Division, School of Engineering, UNAM; Technical Coordinator, IMCYC

It was decided to test the majority of the members under simple bending, a condition representing an extreme case. To evaluate the effects of axial load, two specimens were subjected to combined bending and heavy axial load.

In view of the absence of information of similar tests that would serve as a basis for comparison, the design of the specimens was tentative and limited in size to accommodate the available testing equipment.

It was desired that the members should fail in shear. To achieve this, the preliminary designs were based on the condition that the bending capacity calculated from the Whitney interaction graphs (2) was greater than the capacity calculated for inclined cracking load, assuming that this would occur at a nominal shearing stress, $v_c = 0.5 \sqrt{f'c}$. The actual shear stress was calculated as the quotient of the ultimate shearing force divided by the total area of the section ($v_c = V_c/A_g$).

Except for one case where the size of the specimen was changed, the following characteristics were maintained constant in all other members tested:

- (a) Nominal diameter of the section: 25 cm.
- (b) Length between supports: 210 cm.
- (c) Overhangs: 15 cm.
- (d) Type of steel: LAC DD-40 and wire No. 2 (see Fig. 1)
- (e) Support conditions: Members simply supported with a moveable roller at one end and a fixed roller at the other (Fig. 2).
- (f) Minimum cover: 1.5 cm.

The principal variables were:

- (a) Distribution of the longitudinal steel
- (b) Spacing of stirrups
- (c) Percentage of longitudinal reinforcement
- (d) Compressive strength of the concrete
- (e) Shear span (distance between support and load)
- (f) Axial load

The diameter of the longitudinal reinforcing was considered as a secondary variable.

3. Acknowledgement

This investigation was carried out in the Structural Department of the School of Engineering of the Autonomous National University of Mexico.

The thesis was written as part of the requirements for obtaining the degree of Master of Engineering, under the direction of Roger Diaz de Cossio, Research Scientist and Head of the Doctorate Division of the School of Engineering.

Thanks are expressed to Juan Casillas, Chief Research Scientist, for his suggestions during the planning and development of the program. We also thank Roberto Meli, Javier Mendoza, Mauricio Nanes and Oscar Gonzalez Guevas, Assistant Researchers, for their cooperation during the tests and interpretation of results. Laboratory technicians Antonio Negrete and Jos Zamora rendered efficient assistance during the investigation.

The manuscript was reviewed by Oscar de Buen, Professor of the Doctorate Division, and by Luis Esteva, Research Scientist of the School of Engineering.

4. Notation

The identification of the members and their principal properties are shown in Table 1.

4.1 Dimensions

A_g = area of the cross section of the specimen = $\pi D^2/4$ (sq. cm.)

A_s = area of the longitudinal reinforcement, calculated as a function of the nominal area of the bars (sq. cm.)

A_v = area of two diameters of the transverse reinforcement, calculated as a function of the nominal area (sq. cm.)

a = shear span (cm)

c = distance along the axis of the member from the center of the span to the sections where the electric strain gages were located on the reinforcing bars (cm)

D = diameter of the specimen (cm)

d = distance from the centers of the reinforcement layers to the extreme fiber of concrete under compression (cm)

- L = total length of specimen (cm)
- l = span between supports (cm)
- s = spacing of stirrups (cm)

4.2 Loads and forces

- N = applied axial load (tons)
- V_a = shearing force at crushing of the concrete (tons)
- V_c = shearing force at appearance of an inclined crack (tons)
- V_u = shearing force at maximum load (tons)
- V_y = shearing force at yielding of the lower layer of reinforcing steel (tons)
- V_c' = calculated shearing force carried by transverse reinforcement (tons)
- V_{cc} = calculated shearing force at appearance of an inclined crack (tons)
- V_{uc} = shearing force corresponding to the calculated maximum bending moment (tons)
- V_{yc} = shearing force corresponding to the calculated bending moment at the start of yielding of the longitudinal steel (tons)

4.3 Stresses

- E_{10-50} = secant modulus of elasticity of concrete between 0.1 f_c' and 0.50 f_c' (kg/sq.cm.)
- f_c' = compressive strength of concrete determined from 15 x 30 cm cylinders at the time of testing (kg/sq.cm.)
- f_c'' = 0.85 f_c' (kg/sq.cm.)
- f_t' = tensile strength of concrete determined from the Braxilian test on 15 x 30 cm cylinders at the time of testing (kg/sq.cm.)
- f_y = yield stress of longitudinal steel (kg/sq.cm.)
- f_{vy} = yield stress of transverse steel (kg/sq.cm.)

4.4 Deformations

- Δ = midspan deflections (cm)
- ϵ_c = concrete strain at the extreme fiber in compression
- $\epsilon_o = 2f_c''/E_{10-50}$
- ϵ_s = steel strain

TABLA I PROPIEDADES DE LOS ENSAYOS

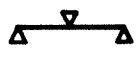
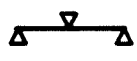
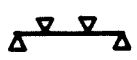
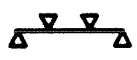
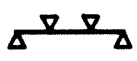
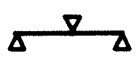
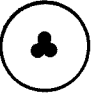
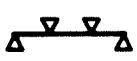
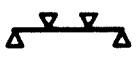
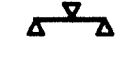
Espécimen	Distribución acero	Tipo de carga	f_c^1 kg/cm ²	D cm	A_g cm ²	P_g %	a/D	s cm	N ton
24.6-2-A B			256 292	24.7 24.6	479.2 475.3	2.12 2.14	4.25 4.26		
25-3-A B			461 444	25.2 25.1	498.8 494.8	3.06 3.08	4.17 4.18		
25-3-C D			299 349	25.1 25.1	494.8 494.8	3.08 3.08	4.18 4.18		61.15 58.30
F-25-3-A B			296 306	25.1 25.2	494.8 498.8	3.08 3.06	2.79 2.38		
F-∞ F-25 F-12.5			134 132 131	25.1 25.1 25.1	494.8 494.8 494.8	3.08 3.08 3.08	2.39 2.39 2.39		25 12.5
F-10 F-6.25			217 216	25.3 24.9	502.7 487.0	3.03 3.13	2.36 2.41	10 6.25	
P-25-3-A B			237 248	25.2 25.1	498.8 494.8	3.06 3.08	4.17 4.18		
P-25-3-C D			249 287	25.2 25.1	498.8 494.8	3.06 3.08	4.17 4.18		
25-3-0			298	25.1	494.8	3.08	4.18		
FU-∞			137	25.1	494.8	3.08	2.39		
F-A			207	25.2	498.8	1.18	2.38		
15-2-A			246	15.1	177.1	2.24	4.17		

TABLE 1 PROPERTIES OF TEST SPECIMENS

II. MATERIALS, SPECIMENS AND INSTRUMENTATION

5. Concrete

The concrete was made from a Type III high early strength Portland cement with 3/4-in. maximum size pea gravel and blue sand from the Santa Fe mines. The screen analysis of the aggregates appears in Table IIa; the values stated are those obtained from an analysis made half way through the test program. The absorption and density data of the aggregates are included in the table.

6. Steel

Proportioning of the concrete was based on previous experience in the laboratory using the same materials.

A 3-1/2 S mixer was used and normal mixing time was three minutes.

Table IIb gives the mix proportions, slump values obtained, f_c' and f_t' , and the age at the time of testing.

The longitudinal reinforcing bars were type LAC-DD-40, No. 4, for all specimens except three, which contained Nos. 2.5, 5 and 8 bars respectively. The stirrups were made from No. 2 wire. Physical properties of the reinforcement were determined from tension tests on coupons taken from each bar and wire lot. The strains were measured up to 0.006 with a Whittemore mechanical strain gage having a standard measuring length of 25.4 cm. From 0.006 to fracture they were measured with a comparison calipers of approximately 0.002 calibration, over the same length.

Table III shows the values of the yield stress of the longitudinal bars used, and the distance from the various bar layers to the extreme fiber under compression of the concrete (d). The yield stress was expressed as that corresponding to a unit deformation of 0.002. Fig. 1 shows typical stress-strain curves of the steel used.

7. Manufacture

All the specimens were cast in cardboard forms except the first two, which were cast in metal forms. The control specimens were cast in rolled steel molds.

The reinforcing bars were the same length as the form so that after casting, their actual position in the member was known. They were tied together with polygonal stirrups in the support and load sections. In addition, in specimens F-6.25 and F-10, stirrups spaced at 20 cm intervals were located

TABLA II a ANALISIS GRANULOMETRICO

AGREGADO	DENSIDAD Ton /m ³	ABSORCION %	% RETENIDO EN MALLAS								MODULO FINURA
			3/4"	3/8"	#4	#8	#16	#30	#50	#100	
ARENA	2.35	7.6	0	0	2.6	12.8	29.9	46.2	61.2	74.1	2.27
CONFITILLO	2.36	4.7	2.7	38.6	95.8	Pasa No. 4 - 4.2				6.37	

TABLE 2a SCREEN ANALYSIS OF AGGREGATE

TABLA II b DISTRIBUCIÓN DE REFORZAMIENTO DE LAS MEZCLAS

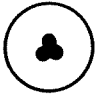
Especímen	Distribución acero	Proporcionamiento en peso				Reveni- miento cm	f' _c kg/cm ²	f' _c kg/cm ²	Edad días
		Agua	Cemento	Arena	Confitillo				
24,6-2-A B		0.66	1	2.65	2.65	3.5	256	20.7	19
		0.66	1	2.65	2.65	4.0	292	25.2	30
25-3-A B		0.48	1	1.50	1.50	7.5	461	34.0	40
		0.46	1	1.50	1.50	7.5	444	26.4	19
25-3-C D		0.66	1	2.75	2.75	8.0	299	25.8	49
		0.66	1	2.75	2.75	10.0	349	27.0	63
F-25-3-A B		0.65	1	2.75	2.75	9.5	296	26.2	26
		0.65	1	2.75	2.75	5.0	306	26.8	28
F-∞		0.90	1	4.45	4.45	15.0	134	14.6	28
F-25		0.90	1	4.45	4.45	13.0	132	16.8	23
F-12.5		0.90	1	4.45	4.45	13.0	131	16.0	25
F-10 F-6.25		0.94	1	4.45	4.45	3.8	217	30.5	28
		0.90	1	4.45	4.45	6.0	216	30.2	26
P-25-3-A B		0.67	1	2.75	2.75	5.5	237	18.9	28
		0.51	1	2.75	2.75	8.0	248	21.4	30
P-25-3-C D		0.62	1	2.75	2.75	10.5	249	22.1	28
		0.60	1	2.75	2.75	11.0	287	25.0	30
25-3-0		0.61	1	2.75	2.75	9.5	298	22.9	28
FU-∞		0.90	1	4.45	4.45	13.0	137	16.0	29
F-A		0.97	1	4.45	4.45	6.5	207	27.9	31
15-2-A		0.67	1	2.65	2.65	2.0	246	23.7	28

TABLE 2b DISTRIBUTION OF REINFORCEMENT, CONCRETE MIX PROPORTIONS AND STRENGTHS

TABLA III DISTRIBUCION Y PROPIEDADES DEL ACERO LONGITUDINAL

Especimen	Distribución acero	Cant. y tam.	A Nominal cm ²		N i v e l							c cm	
					1	2	3	4	5	6	7		
24.6-2-A		8#4	10.16	d	22.5	17.0	8.5	2.7					19
				fy	4130	4130	4150	4150					
B		8#4	10.16	d	22.5	16.3	8.3	2.5					19
				fy	4020	4020	3980	3980					
25-3-A		12#4	15.24	d	23.3	20.8	15.6	9.8	4.4	1.9			19
				fy	3780	3780	4110	4110	3800	3800			
B		12#4	15.24	d	22.7	20.2	15.8	9.6	4.4	1.3			19
				fy	3940	3940	3860	3860	6260	6260			
25-3-C		12#4	15.24	d	23.4	20.7	15.3	10.2	4.9	2.2			6.3
				fy	4170	4170	4090	4090	4020	4020			
D		12#4	15.24	d	23.1	20.3	15.3	9.9	4.7	2.0			6.3
				fy	4040	4040	4090	4090	4060	4060			
F-25-3-A		12#4	15.24	d	23.2	20.6	15.9	10.0	5.0	2.2			fy 60
				fy	4250	4250	4210	4210	4170	4170			
B		12#4	15.24	d	23.0	20.1	15.5	9.9	4.9	1.8			fy 60
				fy	4350	4350	4060	4060	3960	3960			
F-∞		12#4	15.24	d	23.6	20.4	15.7	9.7	4.8	2.3			fy 64
				fy	4090	4090	4450	4450	4170	4170			
F-25		12#4	15.24	d	23.1	20.4	15.3	9.6	5.1	2.4			fy 64
				fy	4090	4090	4130	4130	4130	4130			
F-12.5		12#4	15.24	d	23.1	20.1	15.4	9.6	4.9	2.2			fy 64
				fy	4020	4020	4020	4020	4010	4110			
F-10		12#4	15.24	d	22.8	20.1	15.1	9.4	4.1	2.2			fy 64
				fy	3940	3940	3860	3860	3820	3820			
F-6.25		12#4	15.24	d	22.9	20.3	15.7	9.4	4.0	1.9			fy 64
				fy	4040	4040	3980	3980	3800	3800			
P-25-3-A		12#4	15.24	d	20.0	18.9	6.4	5.3					6.3
				fy	4090	4730	4060	4370					
B		12#4	15.24	d	19.6	18.7	6.6	5.5					25
				fy	4330	4290	4130	3940					
P-25-3-C		12#4	15.24	d	23.0	22.1	15.4	13.1	11.9	3.1	1.8		6.3
				fy	4150	4150	4290	4450	4290	4370	4150		
D		12#4	15.24	d	23.3	21.8	15.5	12.5	12.0	3.4	2.2		25
				fy	3980	3980	4270	4290	4270	4130	3980		
25-3-0		# 8	15.24	d	13.6	11.2							6.3
				fy	4100	4100							
FU-∞		12#4	15.24	d	23.1	22.5	20.7	20.0	15.8	14.6			
				fy	4090	4090	3820	3820	4090	4090			
F-A		3# 8	5.88	d	23.1								
				fy	4190								
15-2-A		8# 2.5	3.96	fy	3920	3920	3920	3920					

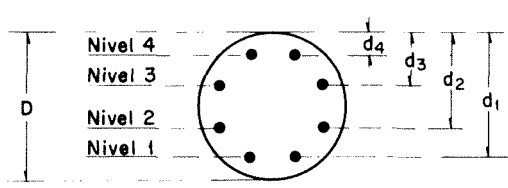


TABLE 3 DISTRIBUTION AND PROPERTIES OF LONGITUDINAL REINFORCEMENT

in the pure bending span. Stirrups at various spaces were located in the shear span (see Fig. 4 and Table 1).

Two batches of concrete were required for each specimen, each batch being carefully mixed to obtain the desired slump. Thorough blending of the concrete was carried out in ten stages. In stages 1, 2, 4, 6 and 8 it was vibrated externally, and in stages 3, 5, 7 and 9, internally. In the tenth and final stage it was vibrated both internally and externally.

Six control cylinders for each specimen were filled in two layers taken from each batch of concrete used in casting the specimens. They were also vibrated internally and externally.

The following day, curing of the specimens was continued by placing wet burlap bags on the upper part. On the third day the forms were removed and the specimens were set down in a horizontal position using the two wire hooks anchored to the reinforcing bars in the upper layer. The specimens were then covered with burlap bags and kept moist until the seventh day.

The control specimens were cured in the same manner as the test specimens.

8. Test equipment

Figures 5-7 illustrate how the loads were applied. The frame for applying the vertical load consisted of two reinforced concrete pedestals each serving as an anchor for two steel bars, 5 cm in diameter. Two transverse beams connected to the steel bars supported one longitudinal beam. The transverse beams were made from two channels bolted together to form a box beam, 30 cm deep. The longitudinal beam consisted of two I beams 38 cm. deep, tied together by 1.25 cm wide plates welded across their flanges.

Concrete pads were placed on top of the pedestals to raise the specimen to a convenient height for testing. Machined steel bearing plates were placed on top of the concrete pads, with a free roller provided at one end and a fixed roller at the other end.

The axial load was applied through a collapsible horizontal frame. The frame was fabricated from rolled steel channels connected by four round steel bars 5 cm in diameter and threaded at the ends. The channels were welded together as shown in Fig. 6. At one end, a plate having a hemispherical depression served as support for a knee joint. At the other end, a 100 ton hydraulic

jack bearing against a flat plate provided the axial load to the specimen through an assembly of parts forming another knee joint.

This horizontal frame was placed so that the specimen was always visible (Fig. 6).

The vertical load was applied by 24 ton hydraulic jacks through machined steel plates connected to reinforced concrete bases as shown in Fig. 2b. Ball type fittings between the jacks and the bearing plates assured vertical loads at all times.

9. Measurements

9.1 Loads

The loads were recorded on manometers connected to the hydraulic system. The manometers were calibrated after every fourth specimen with a calibration box and/or a 100 ton universal Losenhausen machine. It was found that they stayed within the following limits:

100 kg for the 24 ton jacks and

150 kg for the 100 ton jack

9.2 Deflections

The deflections were measured with three Ames dial gages calibrated to 0.01 mm, placed on concrete bases resting on the laboratory floor.

9.3 Strains in the steel and concrete

Strains in the steel and concrete were measured from SR-4 electrical strain gages connected to a Baldwin strain indicator.

The distance, c , of the gages from the center of the specimen is shown in Table III.

9.4 Progressive formation of cracks

The progressive formation of cracks was observed with a lighted magnifying glass. The cracks were sketched with a marker, indicating the number of the load increment at which they appeared. After each load increment the specimens were photographed.

10. Test procedure

10.0 Preparation

During casting of the specimen the reinforcing bars may move or twist slightly, so that symmetry of the steel with respect to the centroid of the

cross-section may not be constant throughout the length of the specimen. A sketch was drawn showing the exact location of the bars at each end of the beam from a line perpendicular to the plane of bending of the beam. A trace showing the location of the longitudinal reinforcing steel was then made on the surface of the specimen and a plane of symmetry determined. The length of the specimen along this plane of symmetry was measured, and at its center a perpendicular circumferential line was drawn. The positions of the support and load points were then located from this center circumferential line. The levels of the end supports were readjusted to compensate for the new position of the longitudinal axis.

After the above procedure on the axial load specimens, the ends of the members were polished and capped with plaster to obtain two plane, parallel faces perpendicular to the longitudinal axis of the specimen.

Aluminum reference points for measuring vertical deflections were cemented to the bottom of the specimen.

A lighted magnifying glass was used to detect cracks due to shrinkage, poor casting procedure, or from any other cause during the test set-up. These cracks were marked accordingly.

After the axial load frame was assembled in position, a sheet of cork was placed between the plaster and the plates, and a small axial load was applied.

For centering the axial load, electric strain gages were placed in four diametrically opposite points 90 degrees apart, and approximately 10 cm from the center of the specimen to measure the strains in the concrete. Dial gages were placed at the center of the span to measure horizontal and vertical displacements of the member. When the radial strains did not vary more than 5 percent, and the horizontal and vertical displacement were each about 0.05 mm under an axial load of about 10 percent of the maximum to be applied, an axial load of approximately one ton was applied so that the end plates and hydraulic jacks could not be dislocated.

Four diameters near the load points were then measured and averaged. The total length was measured and the lengths between supports and loads were checked. Initial readings were then recorded from dial gages and strain gages.

10.2 Application of the load

On the axial load specimens the horizontal load was applied in six increments of 10 tons each and then maintained constant while applying the vertical load.

The vertical load was applied in increments of approximately 10 percent of the calculated capacity until failure occurred.

At each load stage dial gage and strain gage readings were taken. No attempt was made to maintain the load constant between readings. The dial gages were read when the appropriate load stage was reached and again before applying the next increment.

The interval of time between load stages varied from seven to twelve minutes depending on the number of cracks which appeared and the time taken to locate them.

The control specimens were tested either during or immediately after testing of the member.

III. RESULTS

11. Behavior under load and modes of failure

11.1 Behavior

No cracks appeared at the first load stage. During subsequent load stages and until a strain of approximately 0.0003 under tension was reached in the steel in the lower layer, cracks which were nearly vertical appeared first in the region of maximum bending moment, and later in regions where the moment was smaller. Generally the cracks were symmetrical about the midspan. Strains in the reinforcement and deflections at these load stages were proportional to the loads.

As the load was increased, inclined cracks began to form. The existing vertical cracks increased in length, and inclined toward the load points in the shear zones. The changing crack pattern, however, did not produce sudden changes either in the deflections of the beam or in steel strains.

With increased loading a small inclined crack also appeared in one of the shear spans at a distance from the load point approximately equal to the diameter of the beam and located on the longitudinal center line. This crack was sometimes a continuation of a bending crack. At subsequent load stages the slightly inclined crack propagated in two directions, parallel to the reinforcing bars it had crossed.

Generally the appearance of the inclined crack did not occur in any particular section of the member, nor at any particular load. It was therefore not easy to define a visual cracking load. The values given in this paper are those corresponding to the appearance of the inclined crack through which the failure of the member occurred.

In many of the tests, the appearance of the inclined crack occurred simultaneously with the yield of one or more reinforcing bars so that there was a large number of vertical bending cracks. Cracks also developed simultaneously with the crushing of the concrete in some of the members subjected to a single concentrated load. Fig. 8 shows the development of the cracking of specimen P-25-3-A.

The types of failures were very different. In members without web reinforcement, both shear failures, and shear combined with bending failures, occurred. Some shear failures occurred after yielding of the longitudinal steel. In members with web reinforcement shear failures occurred after the stirrups yielded and bending failures occurred with crushing of the concrete and buckling of the longitudinal bars under compression in the pure bending span. In member 25-3-0 the failure was by bond and compression in the upper part of an inclined crack. The modes of failure for all specimens are shown in Table IV.

Photographs after failure of all the specimens tested are shown in Fig. 9.

11.2 Shear Failure

With increasing load, the inclined crack propagated toward the load points, following the path of the longitudinal bars. This effect is clearly seen in specimens P-25-3-C and D (Fig. 9h). Occasionally the concrete collapsed near the load point, as in specimens 24.6-2-A and B, 25-3-A and F-12.5 (Figs. 9a, b, e).

In some cases the failure occurred suddenly with the appearance of the inclined crack, in others it occurred gradually with increasing load. Comparing the values of the maximum load and of the cracking load reported in Table IV, it can be determined for each specimen whether the type of failure was sudden or gradual.

TABLE 4. CALCULATED VS TEST RESULTS

TABLA IV. VALORES MEDIDOS Y CALCULADOS

Especimen	Distribución acero	Tipo de carga	Cortantes Experimentales				Cortantes Calculados				Relaciones Experimental/Calculado					Tipo de Falla
			Vc Ton	Vy Ton	Va Ton	Vu Ton	Vcc Ton	Vyc Ton	Vcc+Vc Ton	Vuc Ton	Vc Vcc	Vu Vcc+Vc	Vy Vyc	Vc Vuc	Vu Vuc	
24.6-2-A B			3.77 *1		4.25	4.65	4.38	2.83		3.67	0.86	1.06		1.03	1.23	C
			4.05	3.80	4.80	4.90	4.61	2.52		3.72	0.88	1.06	1.51	1.09	1.32	C
25-3-A B			6.05	4.03	6.60	7.16	6.21	3.92		5.96	0.97	1.15	1.03	1.02	1.20	C
			5.75	4.26		6.77	6.06	3.78		6.01	0.95	1.12	1.13	0.96	1.12	C
25-3-C D			7.16		7.16	7.16	6.86	5.65		6.09	1.04	1.04		1.18	1.18	F-C
			7.75		7.45	7.75	7.11	5.97		6.76	1.09	1.09		1.14	1.14	F-C
F=25-3-A B			6.30	7.00		7.00	5.76	6.45		8.25	1.09	1.22	1.08	0.76	.85	C
			6.30	7.20		7.70	6.25	7.06		9.45	1.01	1.15	1.02	0.67	.76	C
F=∞			4.75			4.75	4.80	7.21		8.77	0.99	.99		0.54	.54	C
F=25			4.70			5.95	4.77	7.12	6.42	8.40	0.99	.93		0.56	.71	C
F=12.5			5.40	7.10	8.20	8.20	4.75	6.24	8.04	8.25	1.14	1.02	1.14	0.66	1.00	C
F=10 F=6.25			6.50	5.20	9.90	10.3	5.65	6.29	9.80	8.45	1.15	1.05 ³	0.83	0.77	1.22	F
			6.50	6.30	9.90	10.7	5.48	6.50	12.01	8.65	1.19	0.89 ³	0.97	0.75	1.24	F
P=25-3-A B			4.30			4.58	4.69	4.40		4.51	0.92	0.98		0.96	1.01	C
			4.30			4.70	4.73	4.28		4.50	0.91	0.99		0.96	1.04	C
P=25-3-C D			5.40			5.68	4.79	3.70		5.20	1.13	1.19		1.04	1.08	C
			5.30			5.30	5.02	3.54		5.17	1.06	1.06		1.02	1.02	C
25-3=0			3.75		3.20	3.85	5.12	-		2.80	0.73	0.75		1.34	1.38	A-C
FU=∞			5.15	*2		5.90	4.82	-		7.31	1.07	1.22		0.71	0.81	C
F=A			4.80			5.05	4.34	6.00		6.40	1.11	1.16		0.75	0.79	C
15-2-A			1.60	*2	1.82	1.84	1.61	1.00		1.30	0.99	1.14		1.23	1.42	F-C

NOTAS 1 - No se registró por estar la celda defectuosa

2 - Sin celdas

3 - No falló en cortante por lo cual no se considera al calcular los coeficientes -

Promedios 1.01 1.07 1.09

CV % 11 11 18

C = Cortante
F = Flexión

A = Adherencia

In the specimens with stirrups, the inclined crack increased in width slowly, introducing stresses in the stirrups. The maximum load was reached when yielding of the web reinforcement caused spalling of the concrete to expose a considerably deformed reinforcing steel cage (Fig. 9e). The failures by shear occurred in some cases with yielding of the longitudinal steel.

11.3 Bending failure

Specimens 25-3-C and 25-3-D (Fig. 9c) were tested under both vertical and axial load. In both cases, failure in bending due to yielding of the steel and crushing of the concrete was accompanied by a simultaneous shear failure. In 25-3-D failure occurred suddenly, while in 25-3-C the failure was gradual under a sustained load close to the maximum. Members F-10 and F-6-25 (Fig. 9e and f) had stirrups at relatively close spacings and the shear capacity was greater than the bending capacity, so that failure occurred in bending due to crushing of the concrete and buckling of the longitudinal bars in compression, after yielding of the tension steel.

Specimen F-10 was designed so that failure by bending would occur simultaneously with shearing failure. Upon failure by bending the inclined crack opened one millimeter.

11.4 Bond failure

This type of failure was recorded in member 25-3-0 (Fig. 9I), probably as a result of a shearing failure, because the inclined crack clearly formed. The failure by bond was recorded by observing the displacement of the bars at the ends of the specimen. Also, only a few cracks formed, a typical behavior of bond failure.

12. Presentation of results

12.1 Experimental shearing forces

The shearing forces indicated in Table IV do not include the dead weight of the specimen, or the loading equipment, because they were negligible.

The shear force corresponding to collapse of the concrete was determined by visually observing the appearance of a major inclined crack through which failure of the member occurred. This shear could not be verified as a function of the general behavior of the member, as interpreted in the shear-deflection or moment-deformation curves of the steel.

The shearing force at which the lower layer of the reinforcement began to yield was determined when the strains in the bars reached a value of 0.0022 to 0.0025, recorded by the electric strain gages. This shearing force was corrected by taking into account the position of the strain gage, with respect to the center of the span, and multiplying the observed shear by the factor $(L/2 - c)/a$.

The ultimate shearing force was considered to be that corresponding to the maximum load applied during the test. In several specimens failure occurred as the load was being applied.

In Table IV are shown the bending failures (F) the shearing failures (C), and the bond failures (A).

12.2 Deformations

From the recorded data, load-deflection curves for each specimen were drawn, as shown in Fig. 10. In these curves $^{\circ}$ denotes the visual cracking load and * the crushing load.

Strains in the lower layer of the steel for each specimen are plotted as a function of moments in Fig. 11. The moments are computed at the location of the SR4 strain gages, and the strains, $\epsilon_{s\parallel}$, are the average strains recorded for all the bars in layer 1 (Table III). In the same figure (+) marks the moment calculated at the first yielding ($\epsilon_{s\parallel} = 0.0025$).

From load-strain curves of the longitudinal bars, similar to those shown in Fig. 12, and from the recorded strains in the concrete, distribution of steel and concrete strains at various levels of the reinforcement were plotted in Fig. 13 as a function of percentages of maximum load.

Fig. 14 shows shear-strain curves of the transverse steel.

13. Analysis and discussion of results

13.1 Flexural capacity

The maximum bending moment was calculated using Whitney's criterion for ultimate strength design, assuming a strain in the extreme fiber of the concrete under compression of 0.004 and locating the position of the neutral axis by trial and error. Forces in the steel were calculated from the stress-strain diagram using the measured strains in each bar and assuming that the stress-strain curves were identical both in compression and tension.

The moment at the initial yield was calculated when the bars in the lower layer were strained to 0.0025. For the contribution of the concrete a parabolic stress-strain curve (3) was assumed from the expression

$$\frac{f_c''}{f_c'} = \frac{\epsilon_c}{\epsilon_0} \left(2 - \frac{\epsilon_c}{\epsilon_0} \right)$$

where

$$f_c'' = 0.85 f_c'$$

$$E_c = 2 f_c'' / E_{10-50}$$

E_{10-50} = secant modulus of elasticity between
0.1 f_c' and 0.5 f_c'

and

ϵ_c had a maximum value of 1.4 ϵ_0

For the concrete used in this study E_{10-50} was taken as approximately 95000 + 150 f_c' .

The moment at initial yielding of the reinforcement was calculated assuming a linear stress-strain relationship for the secant modulus.

For the specimen with axial load, the shear was calculated from

$$V_{uc} = \frac{P}{2} = \frac{M_{calc} - N \Delta}{a}$$

where

V_{uc} = shear corresponding to the maximum calculated bending moment (ton)

P = applied transverse load (ton)

M_{calc} = bending moment calculated at initial yield or at maximum load (ton)

N = axial load applied (ton)

Δ = deflection in the center of the span (cm)

a = shear span (cm)

From the results it can be seen that the flexural capacity calculated from Whitney's criterion gave conservative values, since some members failed in shear at loads higher than those calculated for failure due to bending (Table IV).

13.2 Strains in the longitudinal steel

The calculated initial yield load was very close to that measured experimentally. In Fig. 11 it is evident that in the centrally loaded members the recorded strains were smaller than those calculated for a given moment. This may be due, among other causes, to the fact that the capacity of the concrete under tension was not considered.

In the members with two loads, however, it is seen that the recorded strains correspond reasonably well with those calculated. For any given moment the strains were greater in the shear span than in the pure bending span. This may be due to the effect of the shear force.

13.3 Plane sections

Fig. 13, obtained as outlined in section 12.2 shows that plane sections do not remain plane when the member is loaded, although this does not affect the calculated flexural load carrying capacity if a linear distribution of strains is assumed.

It is felt however that until a more rational theory is developed for calculating the strength of concrete under diagonal tension in which conditions of compatibility are included, the fact that plane sections do not remain plane after deformation must be taken into account.

13.4 Shear capacity

The expression proposed by the Committee ACI-ASCE 426 on Shear and Diagonal Tension to determine the shear strength of an unreinforced web V_{cc} is

$$\frac{V_{cc}}{bd} = 0.5 \sqrt{f'_c} + 176 p \frac{Vd}{M}$$

where

V_{cc} = shear strength of an unreinforced web

b = width of the section

d = effective depth

f'_c = compressive strength of the concrete measured from control cylinders

p = percentage of longitudinal tension steel (A_s/bd)

V/M = ratio between shear and bending moment in the section in which the shear capacity is calculated.

The expression proposed by the same Committee for the contribution of the stirrups is

$$V_c' = \frac{A_v f_{vy} d}{s}$$

where

V_c' = shear strength of the stirrups

A = total area of the web reinforcement

f_{vy} = yield stress of the stirrup steel

d = effective depth of member

s = spacing of the stirrups

The first expression was obtained from the analyses of experimental results of hundreds of tests on rectangular beams without web reinforcement, and the second is based on the truss analogy of web reinforcement confirmed experimentally by Morsch (4).

To analyze the results of the tests reported in this paper, an attempt was made to utilize these two expressions. For a circular section, however, the terms effective depth, effective area, and steel percentage are not as readily defined as for a rectangular section. Therefore, in analyzing the test data, these parameters were defined in various ways, as follows.

Effective Depth:

- A - From extreme fiber of the concrete under compression to the center of the lower layer of longitudinal reinforcement
- B - From the extreme fiber of the concrete under compression to the centroid of the bars below the center of the cross-section
- C - From the extreme fiber of the concrete under compression to a line which passes through the centroid of the bars in tension at calculated bending failure
- D - Diameter of the section

Steel Area:

- E - Area of all bars below the center of the cross-section
- F - Area of bars in tension at calculated bending failure
- G - Total area of all bars

Effective Area:

- H - That corresponding to effective depth A
- I - That corresponding to effective depth B

J - That corresponding to effective depth C

K - That corresponding to effective depth D

Two ratios, V/M were also considered:

L - At a distance, D, equal to one diameter of the member away from the load point

M - In the middle of the shearing span

The effect of the axial load was taken into account by multiplying the values obtained by the factor $1 + 0.04 N/V$ corresponding to a series of tests (5) where the full axial load was first applied followed by application of the transverse as carried out in this study.

Table V shows the fourteen combinations of parameters studied, the averages of the ratios between experimental and calculated values, and the coefficients of variation of these ratios at inclined cracking load and at failure.

Of all the combinations studied, the expressions

$$V_{cc} = \left(0.5 \sqrt{f_c'} + 176 p \frac{Vd}{M} \right) A_g (1 + 0.04 N/V)$$

$$V_c' = \frac{A_v f_{vy} d}{s} \quad (\text{contribution of the stirrups})$$

proved to be the simplest to apply.

In these expressions the parameters are:

A_g = total area of the transverse section = effective area

A_v = area of two diameters of the transverse reinforcement

d = diameter of cross-section

f_{vy} = yield stress of the transverse steel

p = percentage of steel to total area

V/M = ratio of shear to moment calculated at a distance, D, equal to the diameter of the section, away from the load point

s = spacing of stirrups

With these definitions, the ratios between the experimental and calculated values had an average of 1.01 for the cracking load and 1.07 for the failure load, with an average variation of 11 percent for both cases.

It should be noted (Table V) that the variations at failure were less than at cracking load. This was due mainly to the difficulty in defining the cracking load in the circular sections. Generally a load was taken greater than that which would be obtained by visual inspection of a rectangular section, where the crack is more sharply defined. In members with the longitudinal steel distributed uniformly, and in members with stirrups, the observed inclined crack was formed gradually from a series of small cracks and was not immediately apparent. Even with the uncertainty in defining the inclined cracking load, it was considered essential to include it in the report so that comparisons with other studies could be made. Despite the uncertainty in arriving at the cracking load, the final analysis shown in Table V includes both the cracking and the maximum loads. With only twenty-one specimens tested, no attempt was made to establish a completely separate expression from that proposed by the Committee ACI-ASCE 426. Rather, it was established that the expression proposed for rectangular sections, adequately predicted the shear capacity of the circular test specimens, when the parameters were redefined (Fig. 15).

It can be seen from Table V that with almost any combination of parameters the results obtained are acceptable. However, it should be noted that except for the concrete strength, the other quantities have relatively little influence and therefore do not illustrate much difference in the variation.

It should also be noted that the capacity of the member depends mainly on the total area of the member, rather than the shape of the cross-section, provided it approximately fits a regular polygon (ratios b/d close to 1.0) (6).

It is also conceivable that if all the members used in arriving at the expression proposed by Committee ACI-ASCE 426, were analyzed considering the total area of the section, instead of bd the results might well be similar, since as the embedment length is generally small, d and h become approximately equal. On this basis, a series of specimens identical except for the embedment, might be investigated to establish specifically whether the total area or the effective area bd has more influence on the shearing strength.

TABLE V. COMBINACIONES DE PARAMETROS ESTUDIADOS PARA ANALIZAR LOS RESULTADOS

Comb.	Peralte efectivo				Area de acero			Area efectiva				V/M		V Experimental / V Calculado			
														al agriet. inclinado		a la falla	
	A	B	C	D	E	F	G	H	I	J	K	L	M	Prom.	CV %	Prom.	CV %
1			X			X				X		X		1.51	14	1.58	11
2	X						X	X				X		1.09	11	1.15	11
3		X			X				X			X		1.41	14	1.47	10
4			X			X				X			X	1.44	14	1.51	11
5	X						X	X					X	1.04	11	1.10	9
6		X			X				X				X	1.35	14	1.40	8
7			X			X					X	X		1.16	15	1.21	11
8	X						X				X	X		1.04	11	1.09	10
9		X			X						X	X		1.19	16	1.23	13
10			X			X					X		X	1.12	15	1.17	12
11	X						X				X		X	0.98	11	1.03	10
12		X			X						X		X	1.14	16	1.18	11
13	X				X						X	X		1.15	15	1.19	10
14				X			X				X	X		1.01	11	1.07	11
14'				X			X				X	X		1.02	10	1.07	8

Nota: 14' se obtuvo eliminando en la combinación 14, los especímenes 25-3-0, FU-∞ y FA

TABLE 5 COMBINATION OF PARAMETERS STUDIED IN ANALYZING TEST RESULTS

13.5 Bar diagram

To compare the behavior of the test specimens, a bar diagram was drawn (Fig. 16)* in which the actual capacity of the members, and the contributions of the different factors were considered as percentages of the calculated capacity in bending. Each specimen is represented by two bars. The upper indicates the observed behavior (yield, inclined cracking and crushing of the concrete). The lower bar, with different hatching, indicates the calculated contributions of the concrete, the term pVd/M and the stirrups.

The figure includes the type of load, distribution of the steel, mode of failure and observed cracking pattern.

It is seen from this diagram that the yield of the longitudinal steel under tension does not directly influence the appearance of the inclined cracking and that the capacity beyond the inclined cracking of the specimens without transverse reinforcement varies.

14. Effects of the variables

In the following discussion Fig. 16 will be utilized to analyze some effects of the variables studied.

The conclusions arrived at from the observations of this study are restricted to the number and type of tests made. No attempt to establish a general type of behavior is made or intended.

14.1 Percentage of steel and shearing span

Comparing specimens 24.6-2-A and B and 25-3-A and B, in Fig. 15, which had steel percentage of 2 and 3 percent respectively, it is seen that the effect of the amount of longitudinal steel on the capacity is considerable. Comparing specimens 25-3-A and F-25-3-B in the same figure having ratios Vd/M of 0.29 and 0.66 respectively, it is seen that the increase in capacity is low. From the above observations it may be concluded that of these two parameters the steel percentage has the greater influence. This conclusion justifies an expression similar to that proposed by Watsein (7).

14.2 Distribution of the longitudinal steel

The greater the space between layers of steel, the lower the inclined cracking load. This can be confirmed by comparing specimens P-25-3-A and D, in Fig. 16. It might be assumed that the longitudinal bars had an effect similar to that of horizontal stirrups which carry shear, since the inclined

* Fig. 16 not reproduced.

crack forms from a series of small inclined cracks between layers of bars.

With a larger percentage of compression steel, the inclined cracking load is lower, as can be observed by comparing the members F - ∞ and FU - ∞ . This may be a result of the buckling of the bars under compression and the observation is merely qualitative due to the small number of tests.

14.3 Stirrups

It is seen in Fig. 14 that stresses in the stirrups were observed with the appearance of the inclined crack. In specimens F-25 and F-12.5 the stirrups had only one strain gage. The stirrups were in compression until the inclined crack appeared. Tensile stresses were then observed in the stirrups and it was thought that this effect might arise from bending of the stirrup. In an attempt to prove this, in specimens F-10 and F-6.25, two strain gages were placed on the same stirrup, in the same section, one on the outside and one on the inside. It was found that both stirrups behaved as described above with small variations in strain typical of this kind of measurement.

14.4 Strength of the concrete

Having cast the member vertically, it could be assumed that the strength of the concrete would not be uniform over the entire length. However, in 39 percent of the specimens tested the failures occurred in the bottom part of the member as cast.

The type of support may have affected the location of the failure, as the fixed support was always in the lower part. It is believed, however, that since the specimens were cured horizontally, a fairly uniform strength was obtained over the length of the member.

14.5 Previous cracking

Lengths of some failed specimens were retested, either maintaining the same shearing span, or increasing it, as in F-5.25, which was also inverted. This was done so that failure could be obtained with the available equipment. The load-deflection curves of these specimens are shown in Fig. 10b. Comparing them with those of Fig. 10a, it is noted that the ultimate capacities are not influenced by any appreciable degree by previous cracking.

14.6 Size

Specimen 15-2-A was similar to 24.6-2-A but was only 15 cm in

diameter. All other dimensions of the member scaled down to $2/3$ of specimen 24.6-2A. The load frame was different and the jack for applying the load had a smaller diameter to give the same precision. The beam failed by crushing of the concrete in bending combined with simultaneous shear failure. (See Fig. 9 1 and 10 c.)

Its shear capacity was as calculated indicating that the size seems to have little or no influence. However, further research is necessary before a definite statement can be made.

15. Conclusions

(a) The prediction of the bending capacity using the rectangular stress distribution leads to conservative results. For predicting the bending capacity this does not have much importance, but the small safety margin may result in designing a member which fails in shear even though its calculated flexural capacity may be smaller than its actual flexural capacity. Such was the case with specimens 24.6-2-A and B, 25-3-C and D, P-25-3-B, P-25-3-C, 25-3-0, 15-2-A in this study.

(b) The expression proposed by ACI-ASCE-426, with the parameters redefined as in section 13.4, is adequate for evaluating the shear capacity of circular sections without transverse reinforcement, and having the longitudinal steel distributed uniformly around the cross-section.

(c) The shearing strength depends primarily on the strength of the concrete, on the total area of the cross section and, for the combinations of variables studied, a little on the percentage of longitudinal steel and slightly less on the term Vd/M .

(d) The contribution of the stirrups in the shear strength can be adequately estimated by the analogy of Morsch, $A_v f_{vy} d/s$, with d as the diameter of the section.

IV. DESIGN RECOMMENDATIONS

Due to the small number of specimens tested, it is necessary to propose a conservative recommendation. Therefore, the recommendations set forth here are applicable to the following conditions:

Percentage of steel: 1 to 3 percent

Strength of the concrete: 130 to 46 kg/sq.cm.

Ratios of embedment to diameter $1/12$ to $1/10$

Steel distributed uniformly in the cross-section

With these conditions, the suggested amendments to the paragraph relating to the Official Draft of the Regulations for Construction of the Federal District and to ACI-318-63, are shown underscored in the Appendix, redefining the parameters for a circular section.

With respect to the effect of the axial load, the two codes consider different expressions from those analyzed in this paper. However, in applying them to the two specimens reported here, satisfactory results were obtained.

V. REFERENCES

1. Committee ACI-ASCE-426, "Shear and Diagonal Tension", ACI Journal, January, February, March 1962.
2. C. S. Whitney and E. Cohen, "Guide for Ultimate Strength Design of Reinforced Concrete", ACI Journal, November 1956.
3. E. Hognestad, N. W. Hanson, and D. McHenry, "Concrete Stress Distribution in Ultimate Strength Design", ACI Journal, December 1955.
4. E. Morsch, "Theory and Practice of Reinforced Concrete", Vol. II, Spanish translation of G. Gili Editor, Barcelona, 1948.
5. R. Diaz de Cossio, C. P. Siess, "Strength and Behavior of Reinforced Concrete Beams and Frames", University of Illinois, Civil Engineering Studies, Structural Research Series No. 163, Urbana, Illinois, September 1958.
6. M. J. Faradji, "Effects of Size and Form on the Resistance to Diagonal Tension of Beams of Reinforced Concrete Without Web Reinforcement", Instituto de Ingenieria, U.N.A.M., July 1961.
7. R. G. Mather, D. Watsin, "Shear Strength of Beams Without Web Reinforcement Containing Deformed Bars of Different Yield Strength", ACI Journal, February 1963.

APPENDIX I

Proposed amendments to the Official Draft of the Regulations for
Constructions in the Federal District.

Note: The amendments or additions are underlined.

Article 227. Diagonal tension

I. Shearing Stress

The average shearing stress in a section shall be calculated from
the expression $v = V/bd$ or $v = \underline{V/A_g}$ for circular sections. ($A_g = \pi D^2/4$ where
D is the diameter of the section.)

II. Permissible shearing stress in the concrete

a) In sections subjected to bending without axial load the average
shearing stress carried by the concrete shall not exceed

$$v_c = 0.25 \sqrt{f_c'} \quad (3)$$

The effect of the longitudinal steel may be taken into account
using the expression

$$v_c = 0.25 \sqrt{f_c'} + 90 A_s V/bM \quad (4a)$$

or

$$v_c = 0.25 \sqrt{f_c'} + 90 A_s/A_g VD/M \quad (4b)$$

for circular sections.

When b/d differs appreciably from $1/2$, the second member of equations
3 and 4a must be multiplied by $\sqrt{0.4 (2 + b/d)}$. In no case shall v_c be taken
greater than $0.5 \sqrt{f_c'}$.

b) In sections subjected to combined flexure and compression, the
permissible stress calculation according to section (a) may be increased by
multiplying it by $(1 + 0.05 N/V)$.

c) In sections subjected to combined flexure and tension, the per-
missible stress calculated according to section (a) must be reduced by
multiplying it by $(1 - 0.5 N/N_o)$.

IV. Web reinforcement in beams and columns

When v is greater than v_c , web reinforcement is required to carry
the excess. Spacing of the stirrups shall not exceed

$$s = 0.75 A_v f_s d (\sin \theta + \cos \theta) V' \quad (5)$$

and should not be greater than

$$(a) \quad d (1 + \cot \theta) V_c$$

$$(b) \quad 0.5 d(1 + \cot \theta)$$

$$(c) \quad L/6$$

where

$$V' = V - V_c$$

A_v = area of stirrups

$$f_s \leq 1265 \text{ kg/sq.cm for structural grade steel}$$

$$= 0.5 f_y \text{ for other steels}$$

θ = angle which the reinforcement makes with the axis of the member and shall lie between 30° and 90°

For circular sections d shall be replaced in the expressions by D (D = diameter of the section).

No stirrups shall be accepted which form an angle θ less than 45° except when they are adequately welded to the longitudinal reinforcement.

APPENDIX II

Proposed amendments to Regulation ACI-318-63.

Note: The amendments or additions are underlined. Only those sections affected by the proposed amendments are shown.

Chapter 17. Shear and diagonal tension

Ultimate design

A_g = gross area of the section

A_s = area of tension reinforcement or area of the total reinforcement for members of circular sections

$p_w = A_s/b'd$ or A_s/A_g for circular sections

v_c = shear stress carried by the concrete

V_u = total ultimate shear

v_u = nominal ultimate shear stress as a measure of the diagonal tension

1701. Maximum shear strength

(a) The nominal ultimate shearing stress, as measure of the diagonal tension in reinforced concrete members shall be computed

$$v_u = V_u/bd \quad (17-1)$$

For design, the maximum shear shall be considered as that at the section a distance d from the face of the support. Wherever applicable, effects of torsion shall be added and the effects of inclined flexural compression in variable depth members shall be included.

(b) For I-or T-section, b' shall be substituted for b in Eq. (17-1) and for circular sections bd shall be substituted for $\underline{A_g} = IId^2/4$.

Main Reinforcement
No. 4 Bars

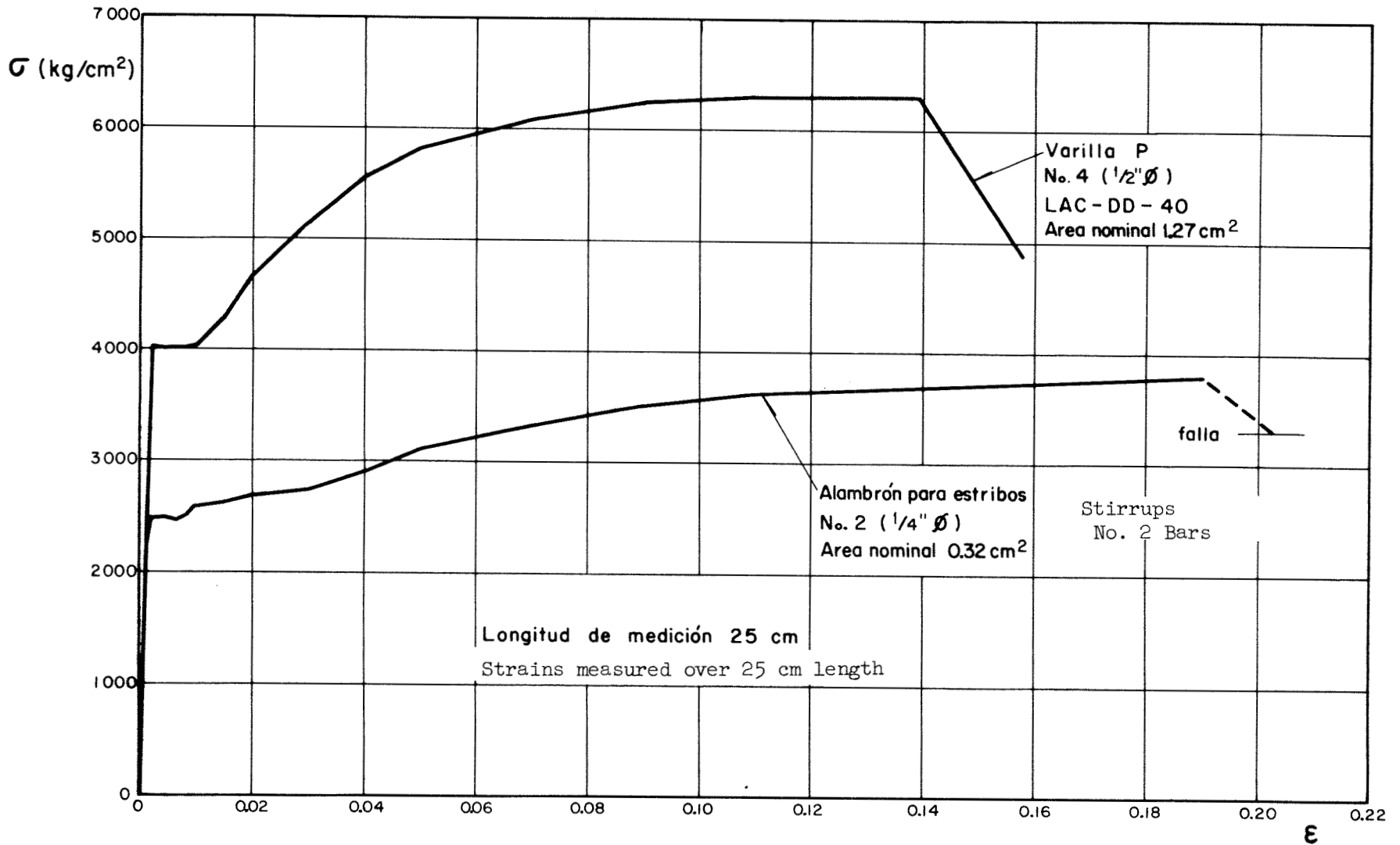
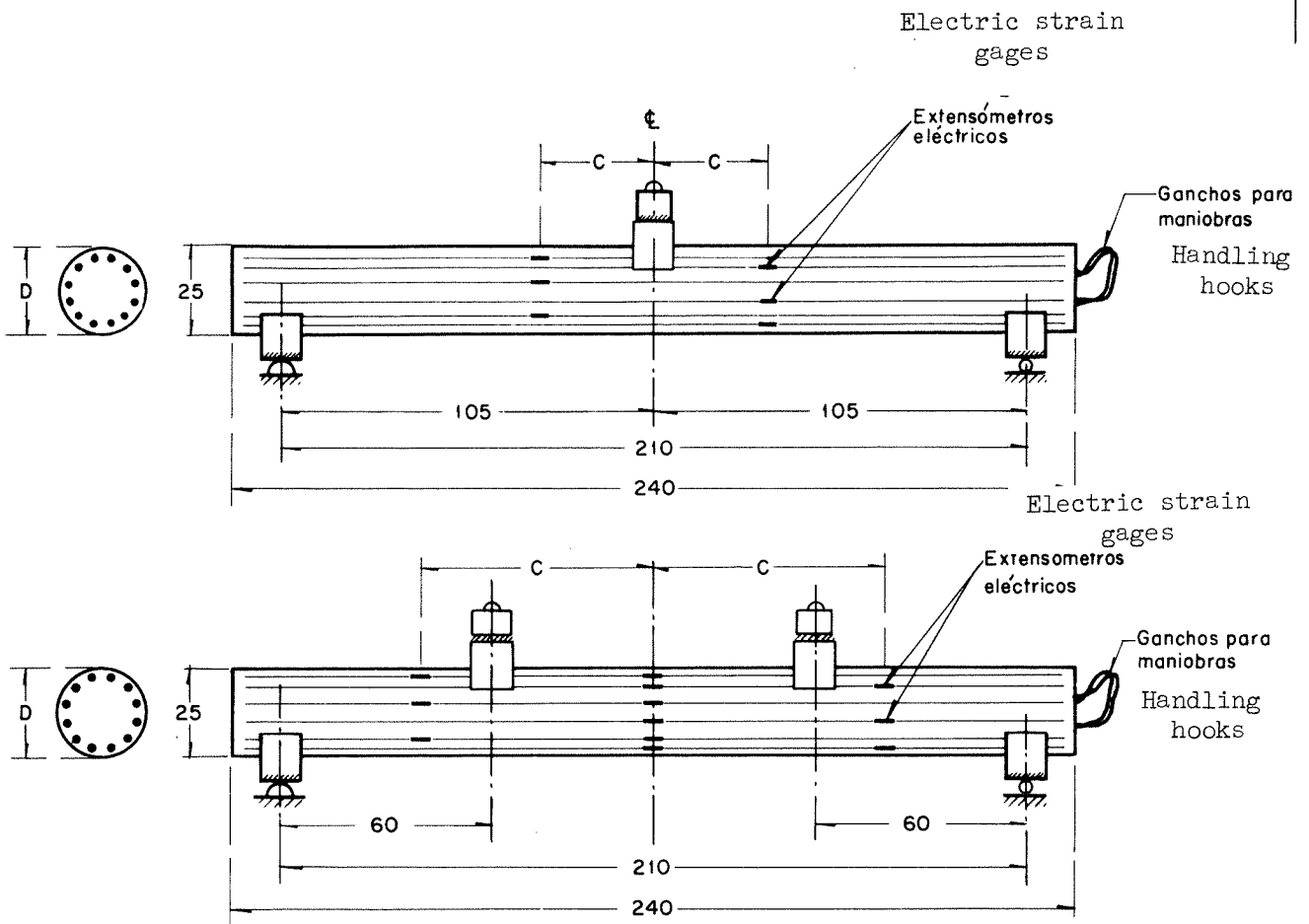
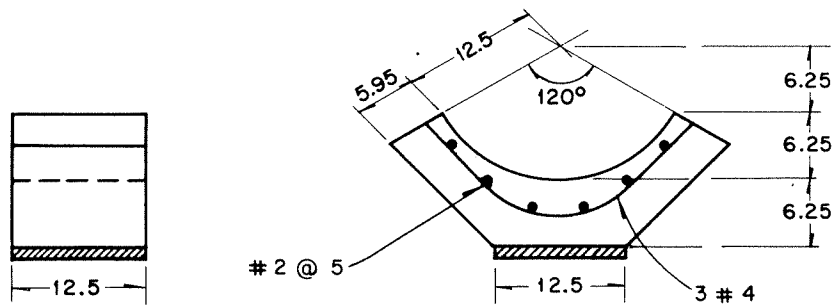


FIG. 1 CURVA TÍPICA DE FLECHA DEFLECTIVA EN UNIDAD DE ELONGACIÓN EN EL ACERO EMPLEADO
FIG. 1 TYPICAL STRESS-STRAIN CURVES FOR REINFORCING STEEL



a) Croquis de los especímenes ensayados
Sketch of test specimen



b) Zapatas de apoyo y carga
Details of load and support shoes

FIG. 2 CARACTERISTICAS GENERALES DE LOS ESPECIMENES

FIG. 2 GENERAL DETAILS OF SPECIMENS

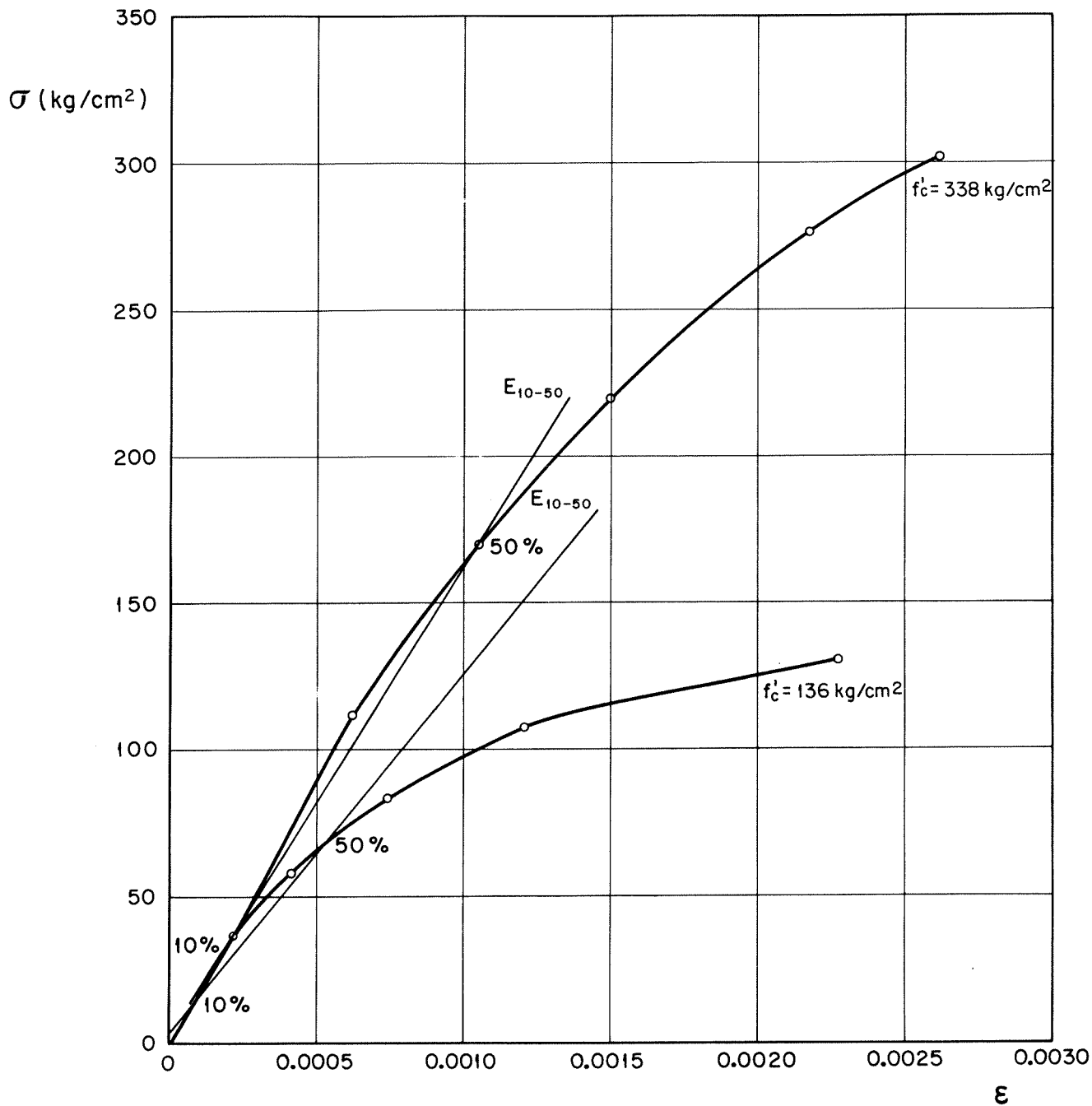


FIG. 3 CURVAS TÍPICAS ESFUERZO-DEFORMACION UNITARIA DEL CONCRETO EMPLEADO.

FIG. 3 TYPICAL STRESS-STRAIN CURVE OF CONCRETE USED

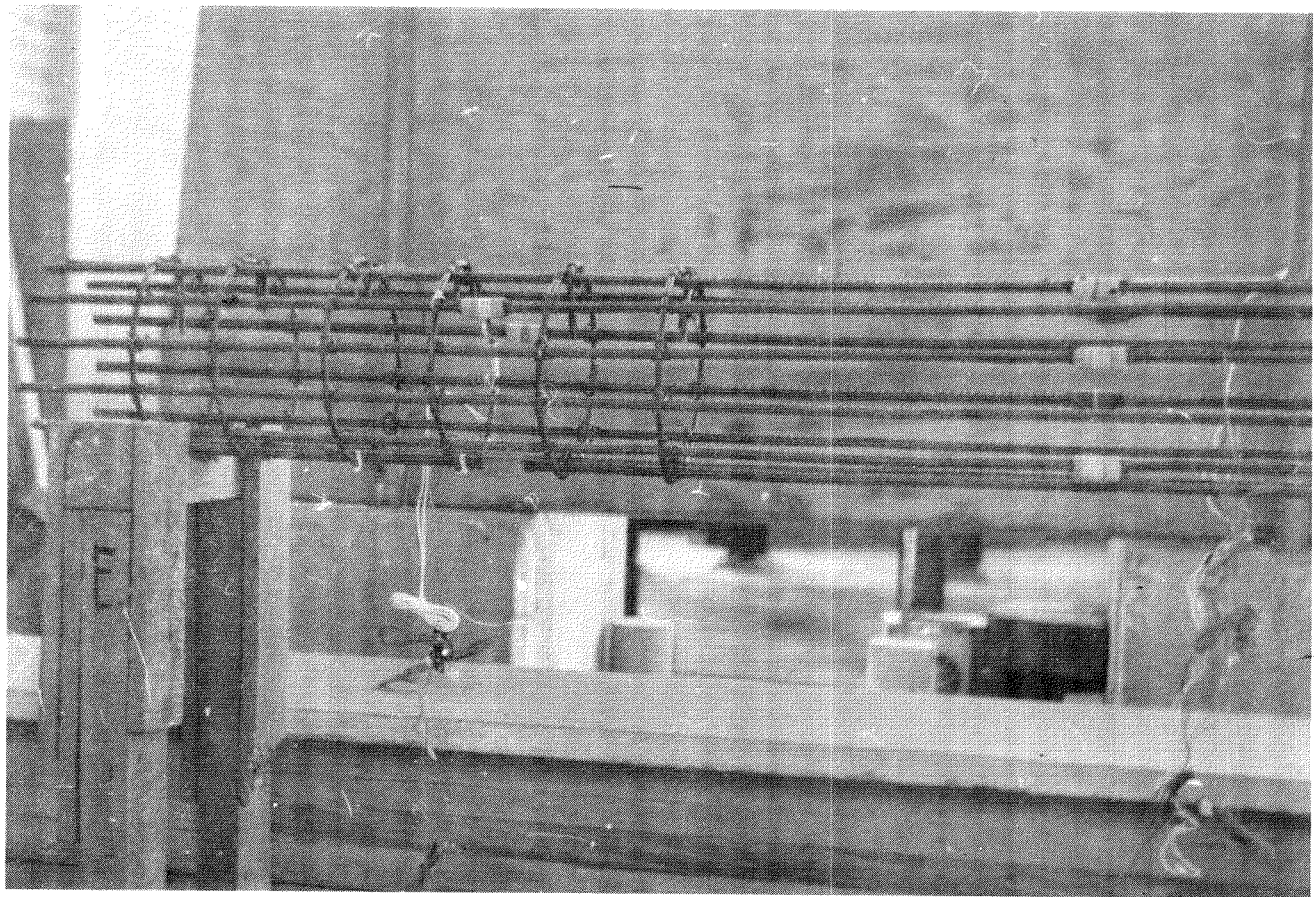


Fig. 4. Aspecto de un armado (nótese la colocación de los
extensómetros eléctricos).

FIG. 4 VIEW OF REINFORCING CAGE FOR ONE SPECIMEN
(NOTE LOCATION OF ELECTRIC STRAIN GAGES)

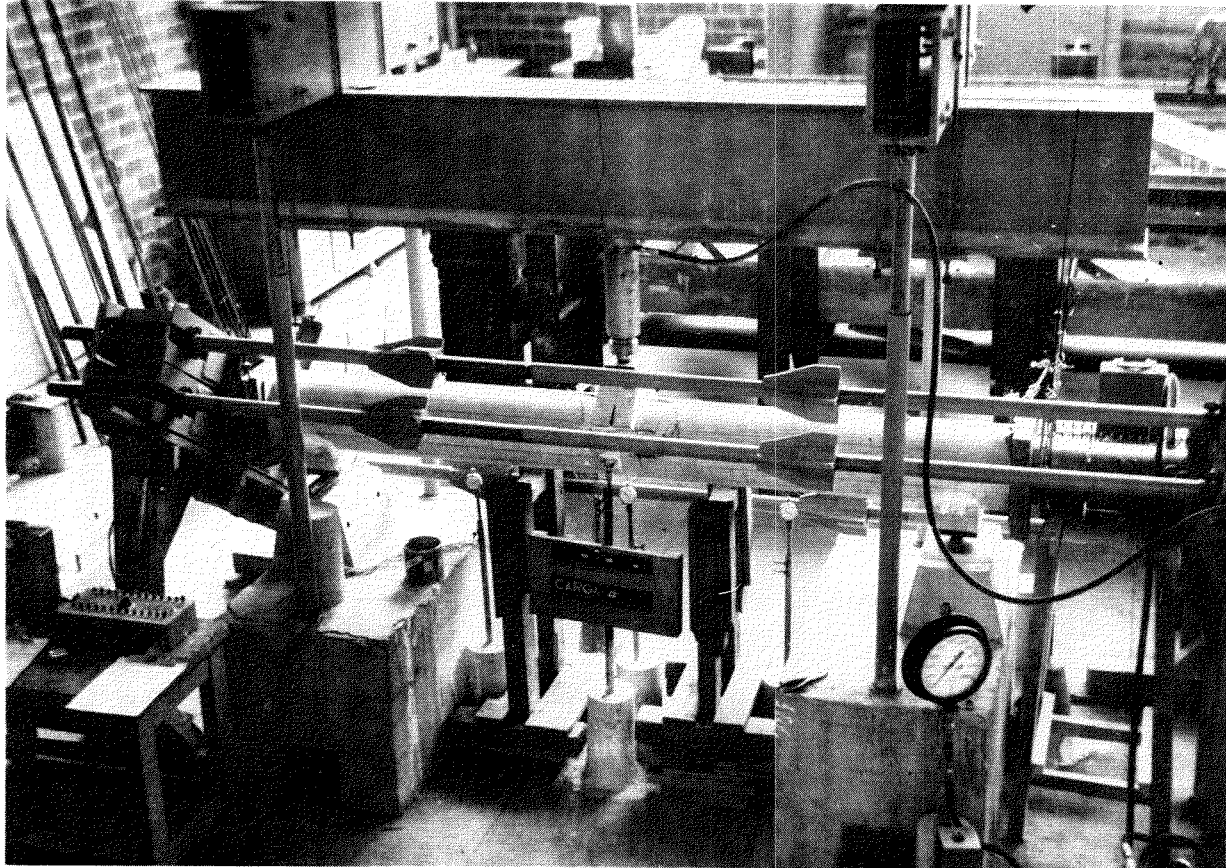


Fig. 5. Vista general del marco de carga

FIG. 5 FRONT VIEW OF LOADING FRAME

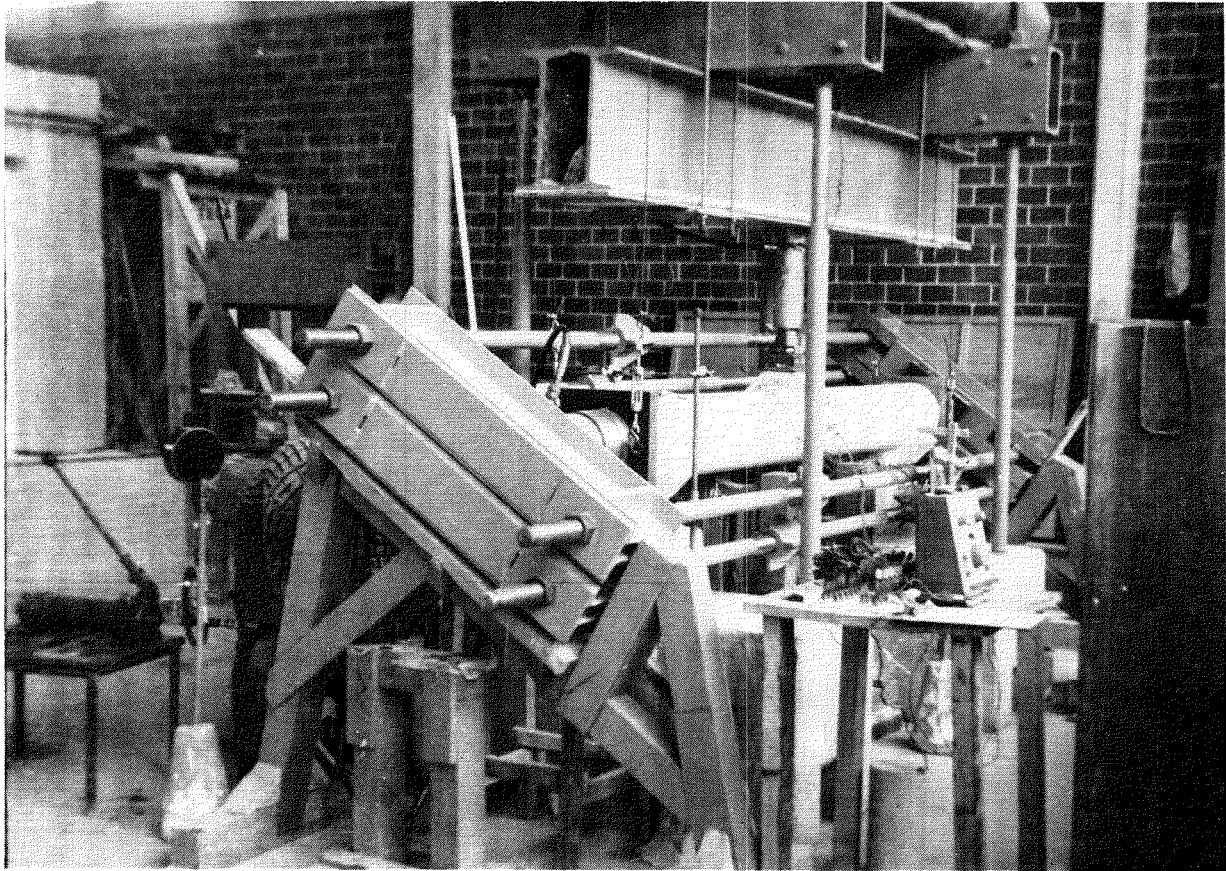


Fig. 6. Vista lateral del marco de carga

FIG. 6 SIDE VIEW OF LOADING FRAME

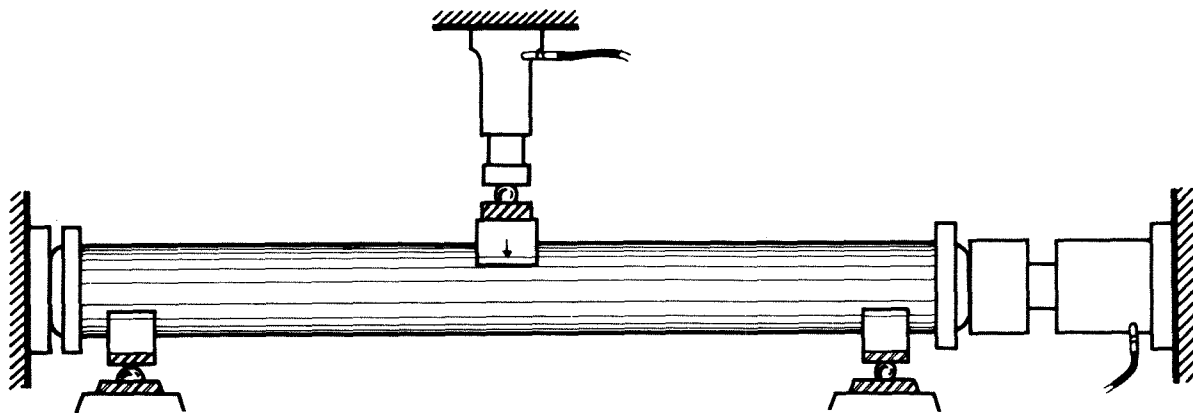


FIG. 7 ESQUEMA DE ELSAYE

FIG. 7 TEST SET-UP

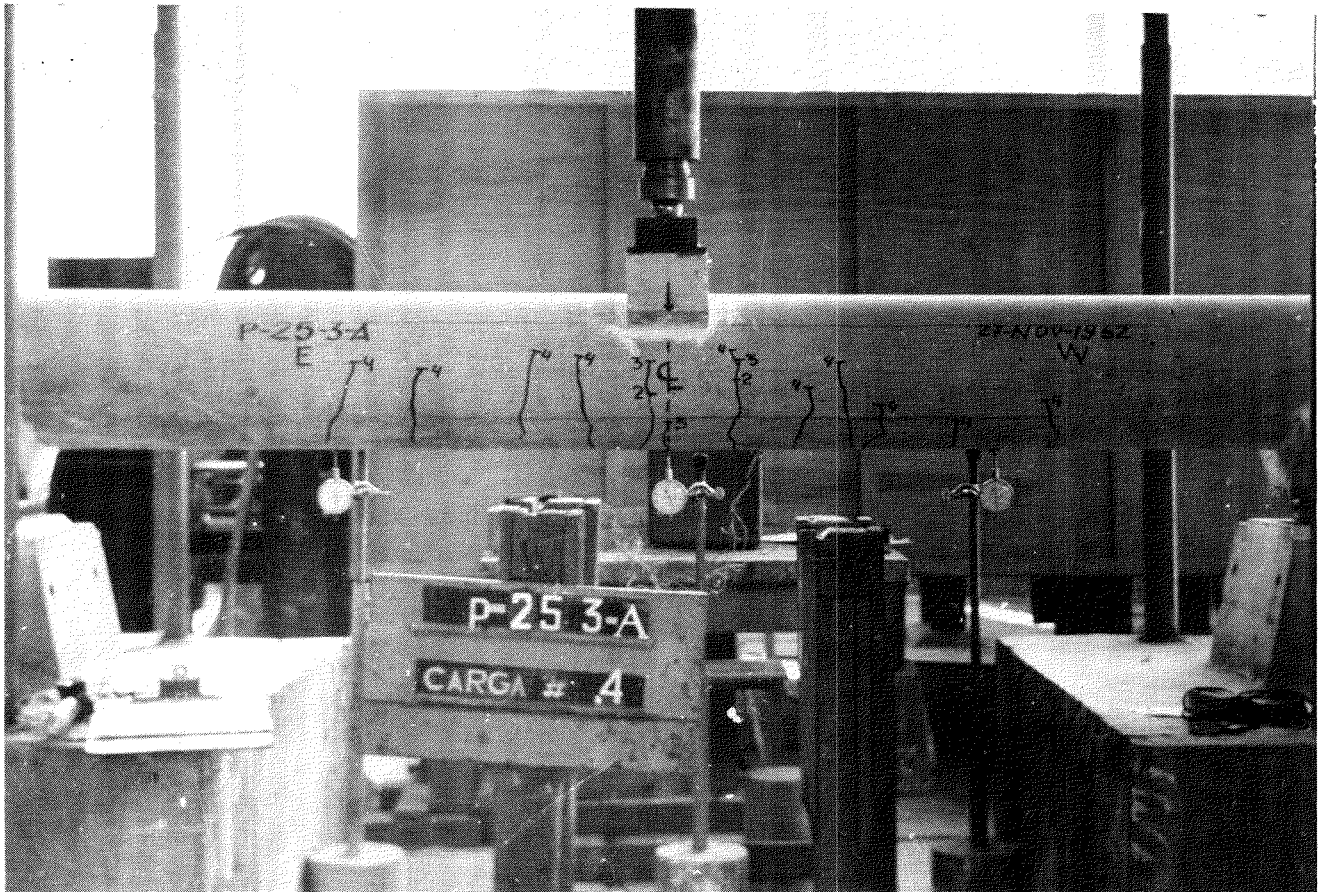
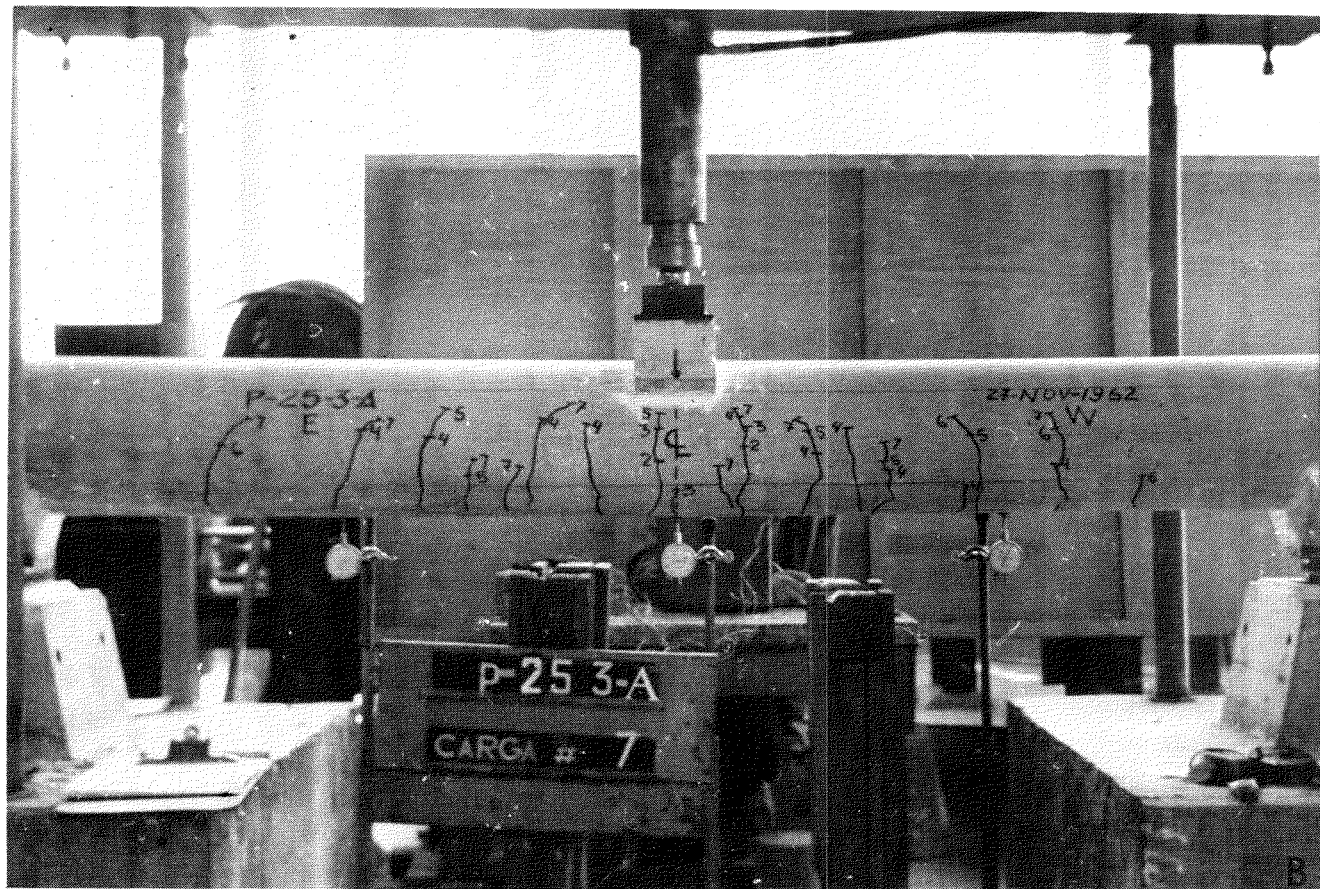


Fig. 8a. Desarrollo de agrietamiento en el espécimen P-25-3-A.

FIG. 8a DEVELOPMENT OF CRACKS IN SPECIMEN P-25-3-A



**Fig. 8b. Desarrollo de agrietamiento en el espécimen
P-25-3-A (continuación)**

FIG. 8b DEVELOPMENT OF CRACKS IN SPECIMEN P-25-3-A (continued)

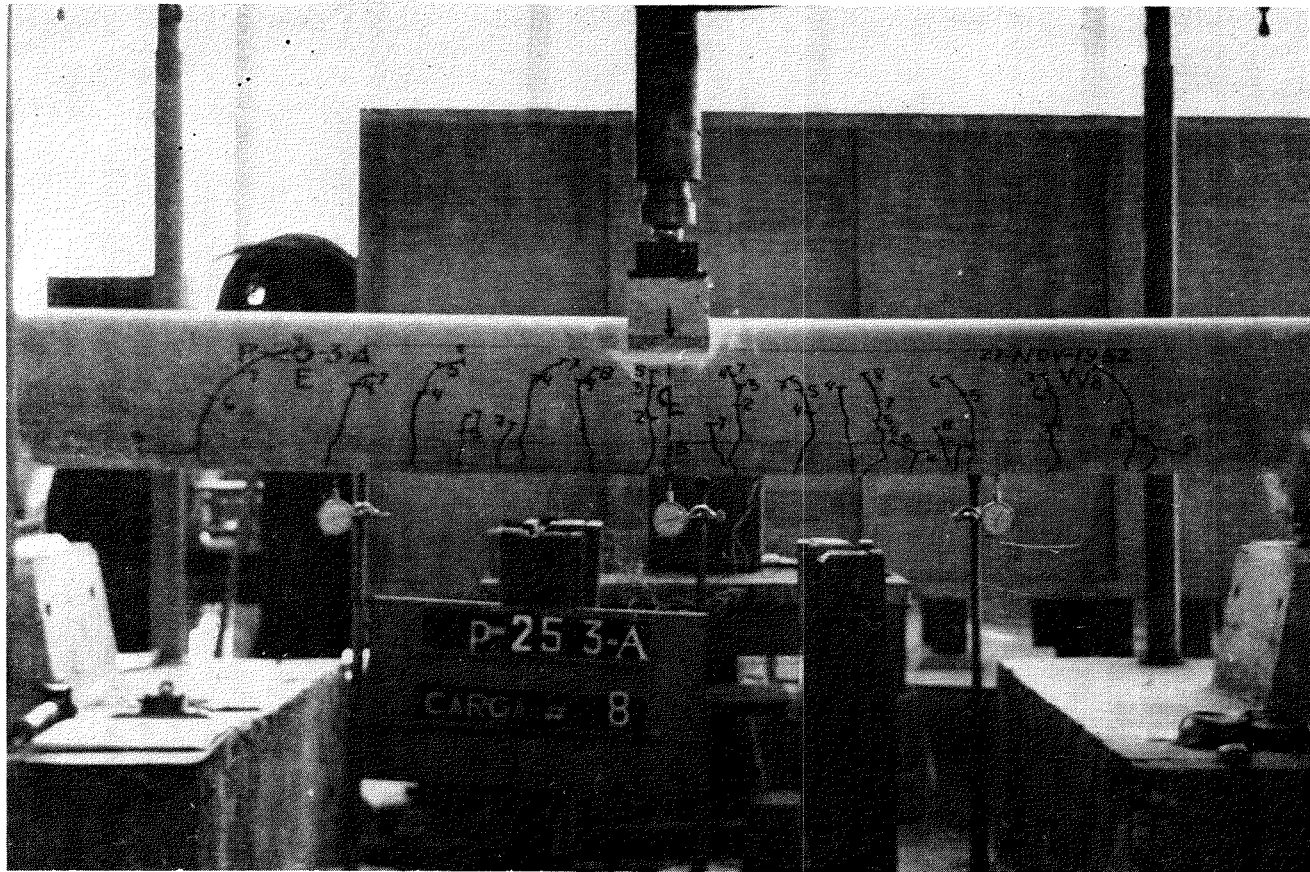
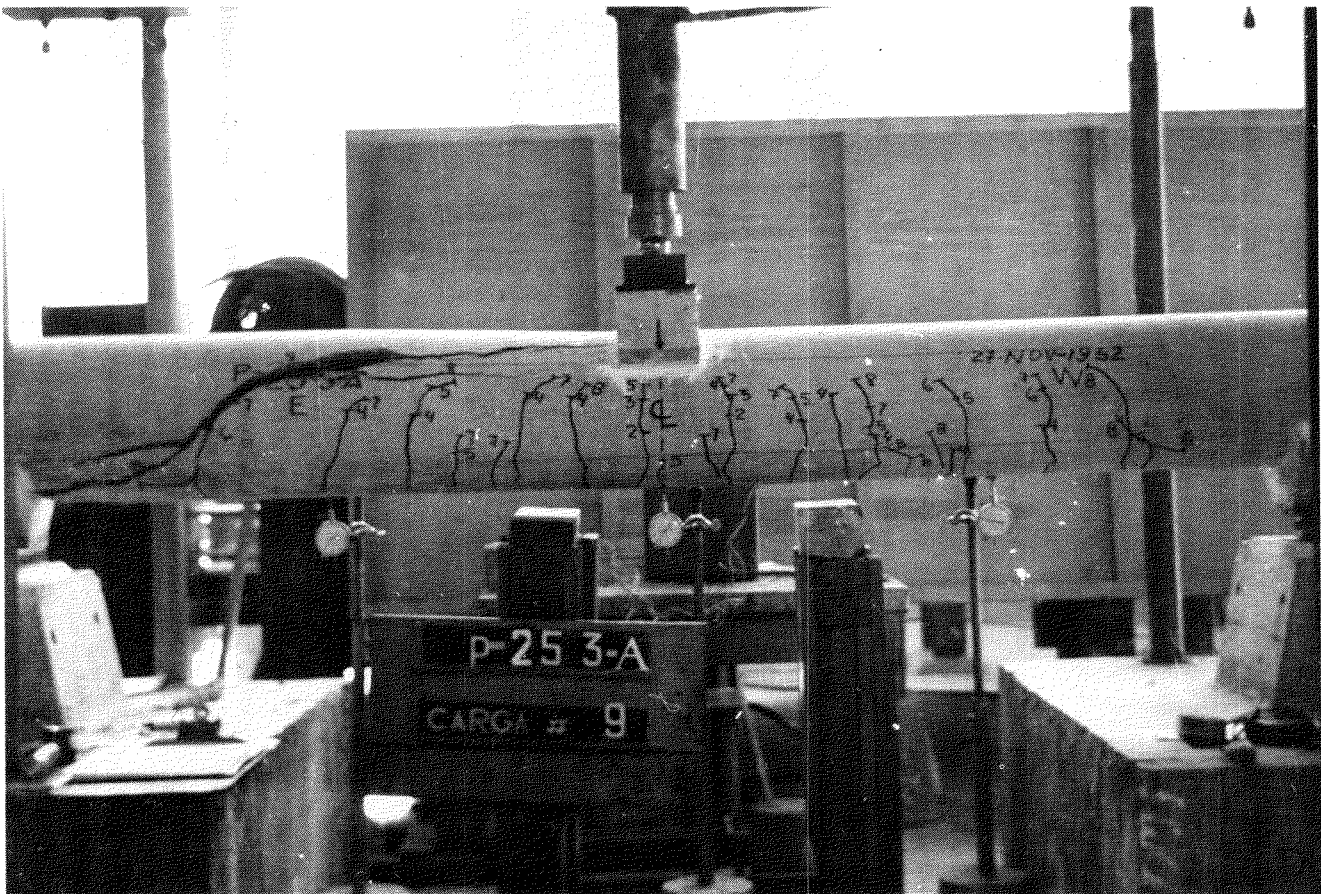


Fig. 8c. Desarrollo de agrietamiento en el espécimen P-25-3-A. (continuación)

FIG. 8c DEVELOPMENT OF CRACKS IN SPECIMEN P-25-3-A (continued)



**Fig. 8d. Desarrollo de agrietamiento en el espécimen
P-25-3-A. (continuación)**

FIG. 8d DEVELOPMENT OF CRACKS IN SPECIMEN P-25-3-A (continued)

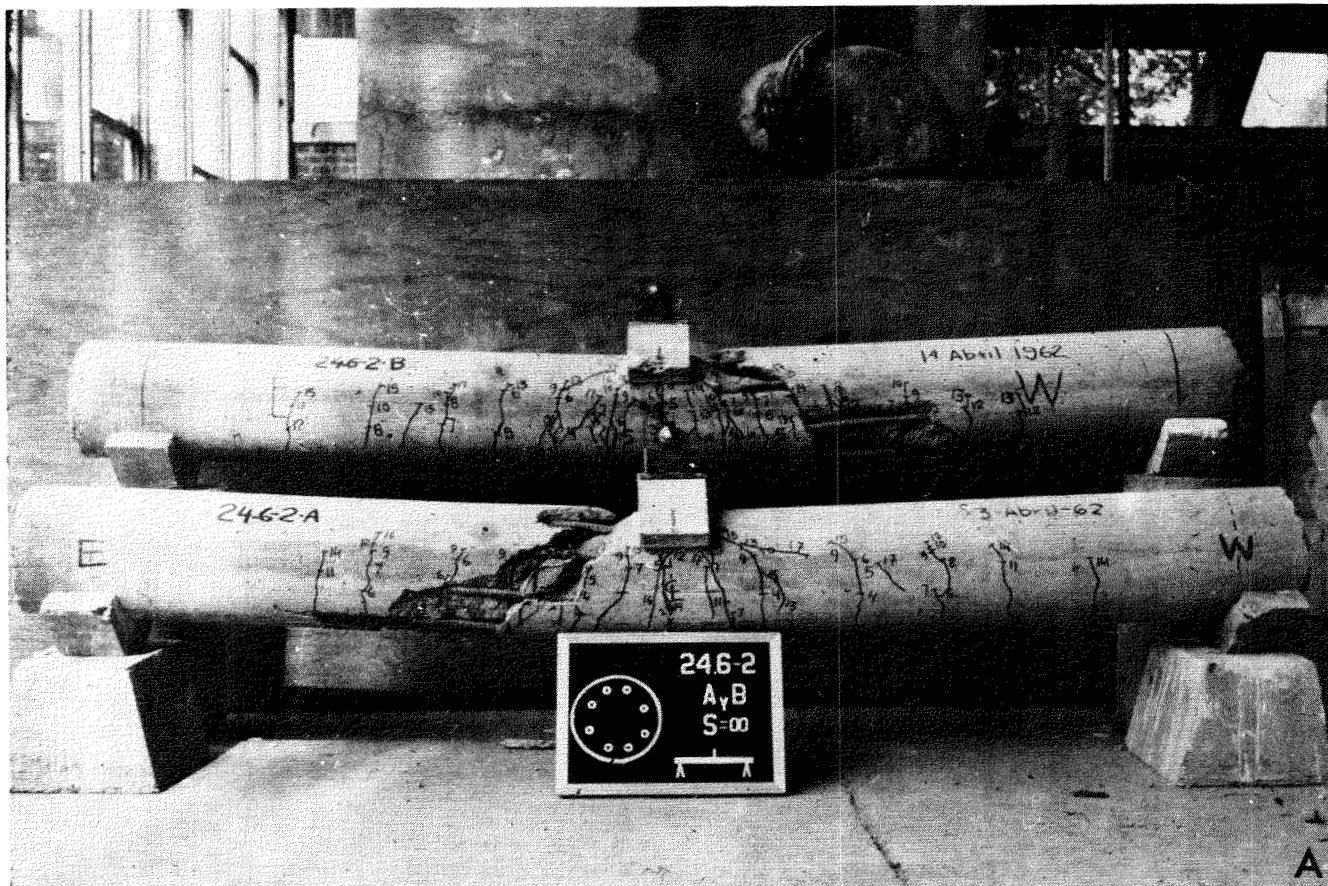


Fig. 9a. Especímenes después de la falla.

FIG. 9a PHOTOGRAPHS OF SPECIMENS AFTER FAILURE.

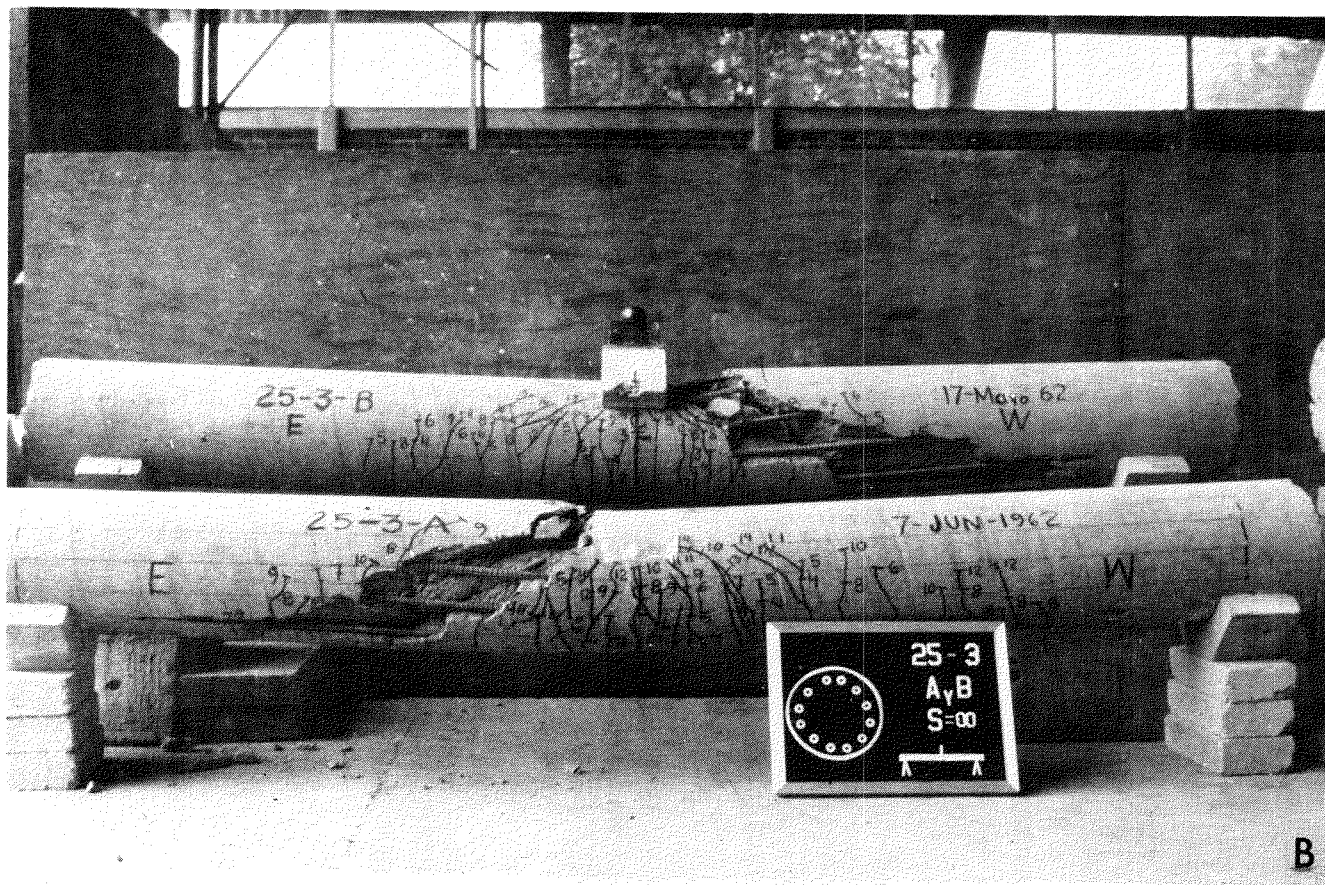


Fig. 9b. Especímenes después de la falla (continuación)

FIG. 9b PHOTOGRAPHS OF SPECIMENS AFTER FAILURE (continued)

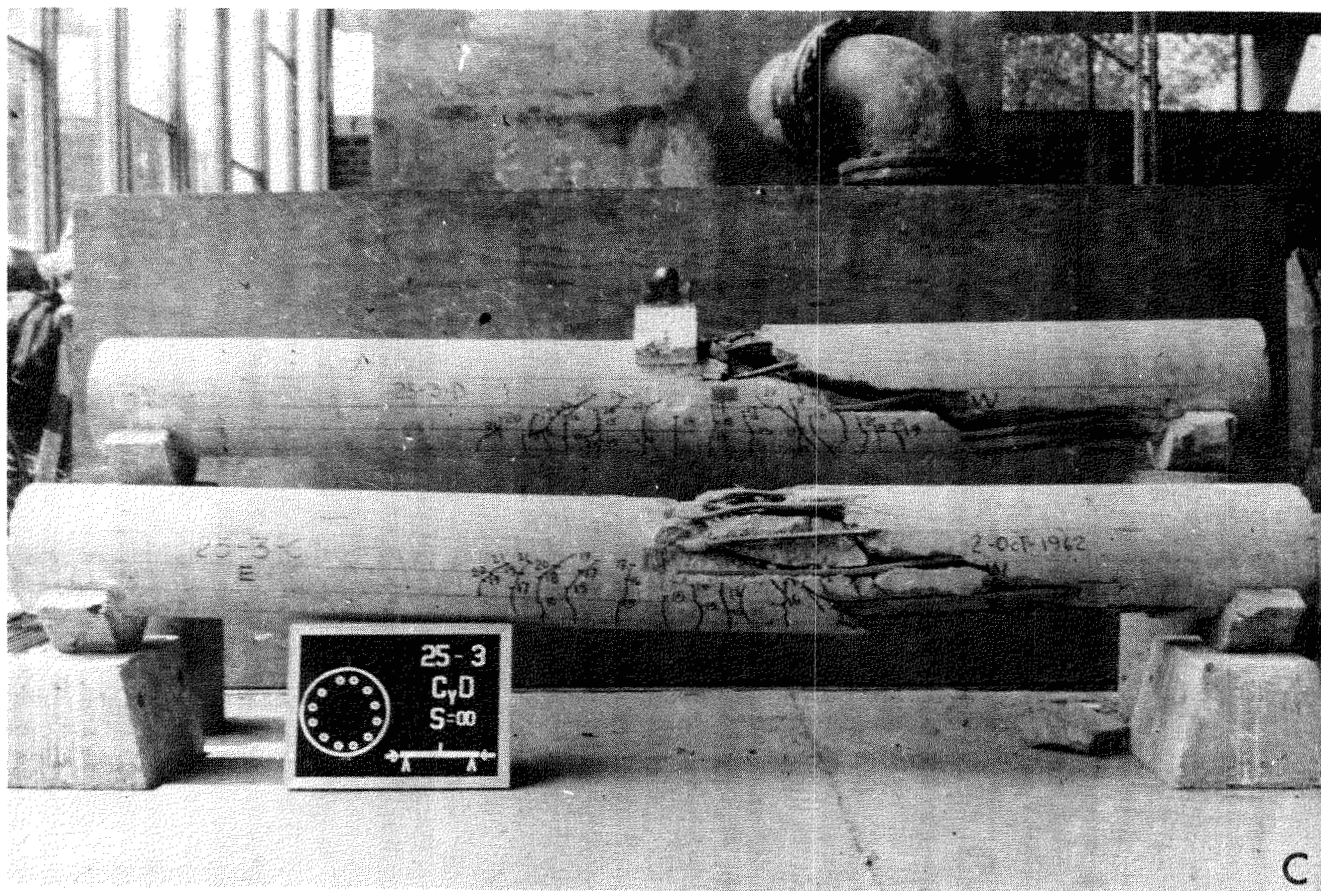


Fig. 9c. Especímenes después de la falla (continuación)

FIG. 9c PHOTOGRAPHS OF SPECIMENS AFTER FAILURE (continued)

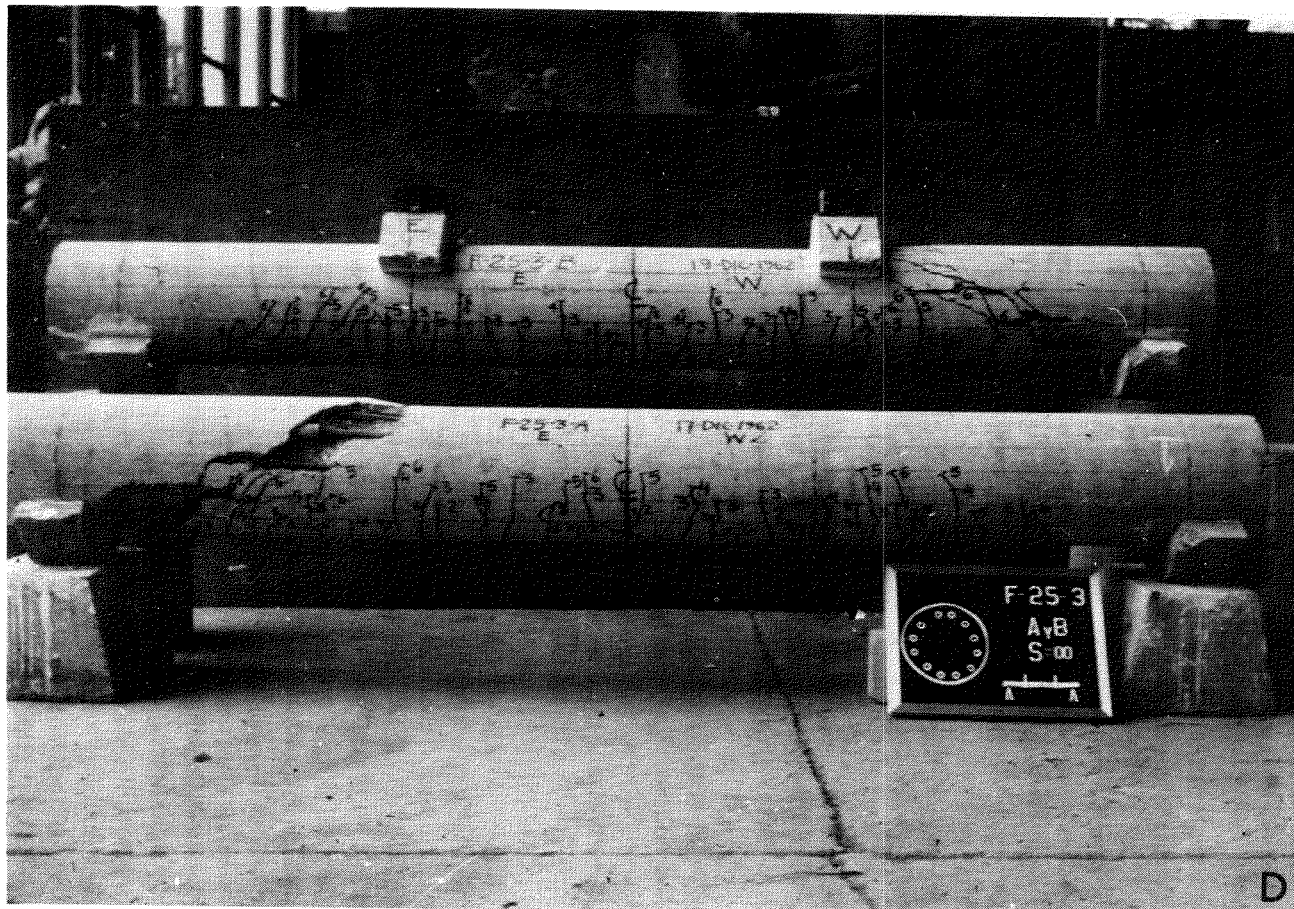


Fig. 9d. Especímenes después de la falla (continuación).

FIG. 9d PHOTOGRAPHS OF SPECIMENS AFTER FAILURE (continued)



Fig. 9e. Especímenes después de la falla. (continuación)

FIG. 9e PHOTOGRAPHS OF SPECIMENS AFTER FAILURE (continued)

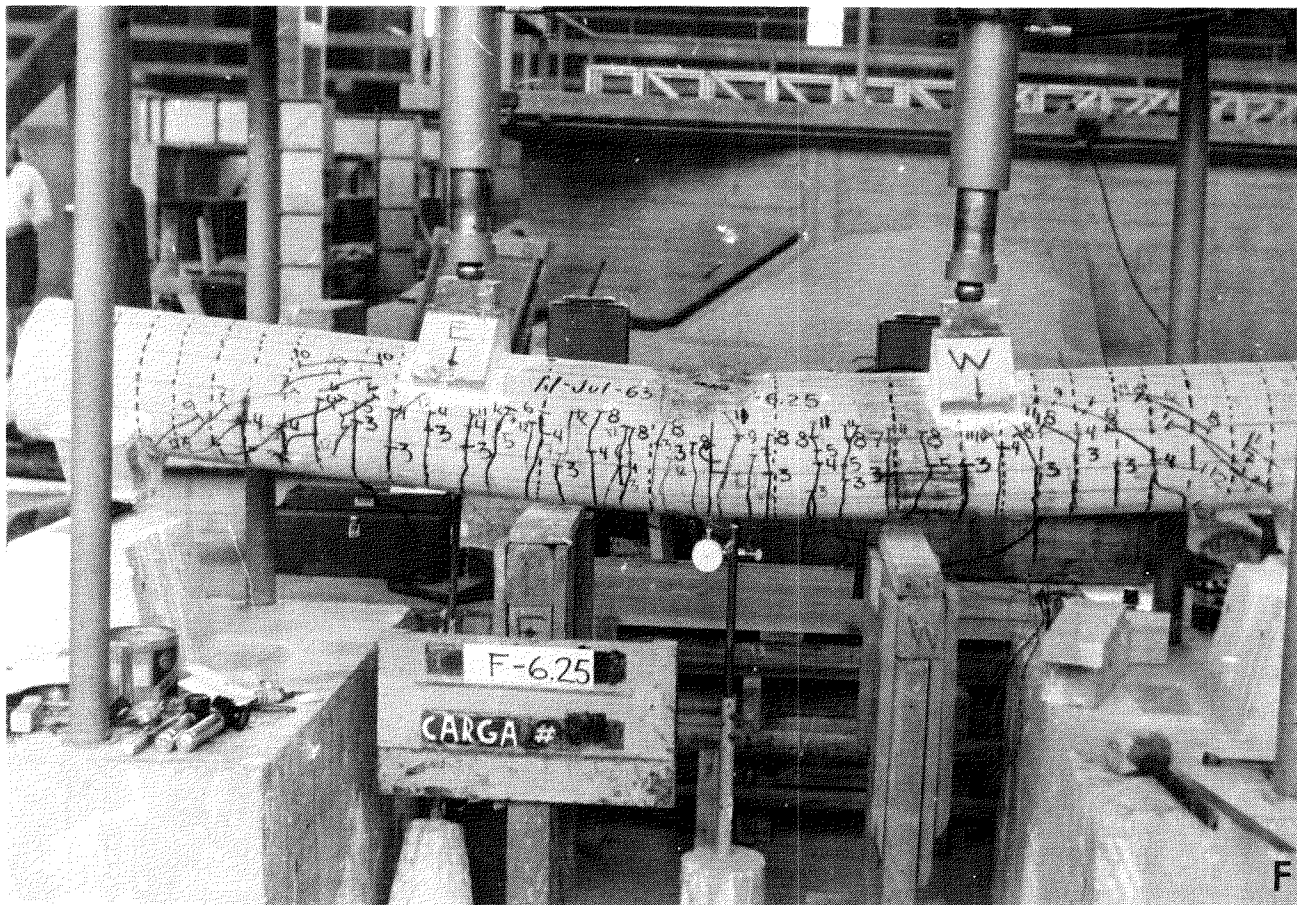


Fig. 9f. Especímenes después de la falla. (continuación)

FIG. 9f PHOTOGRAPHS OF SPECIMENS AFTER FAILURE (continued)

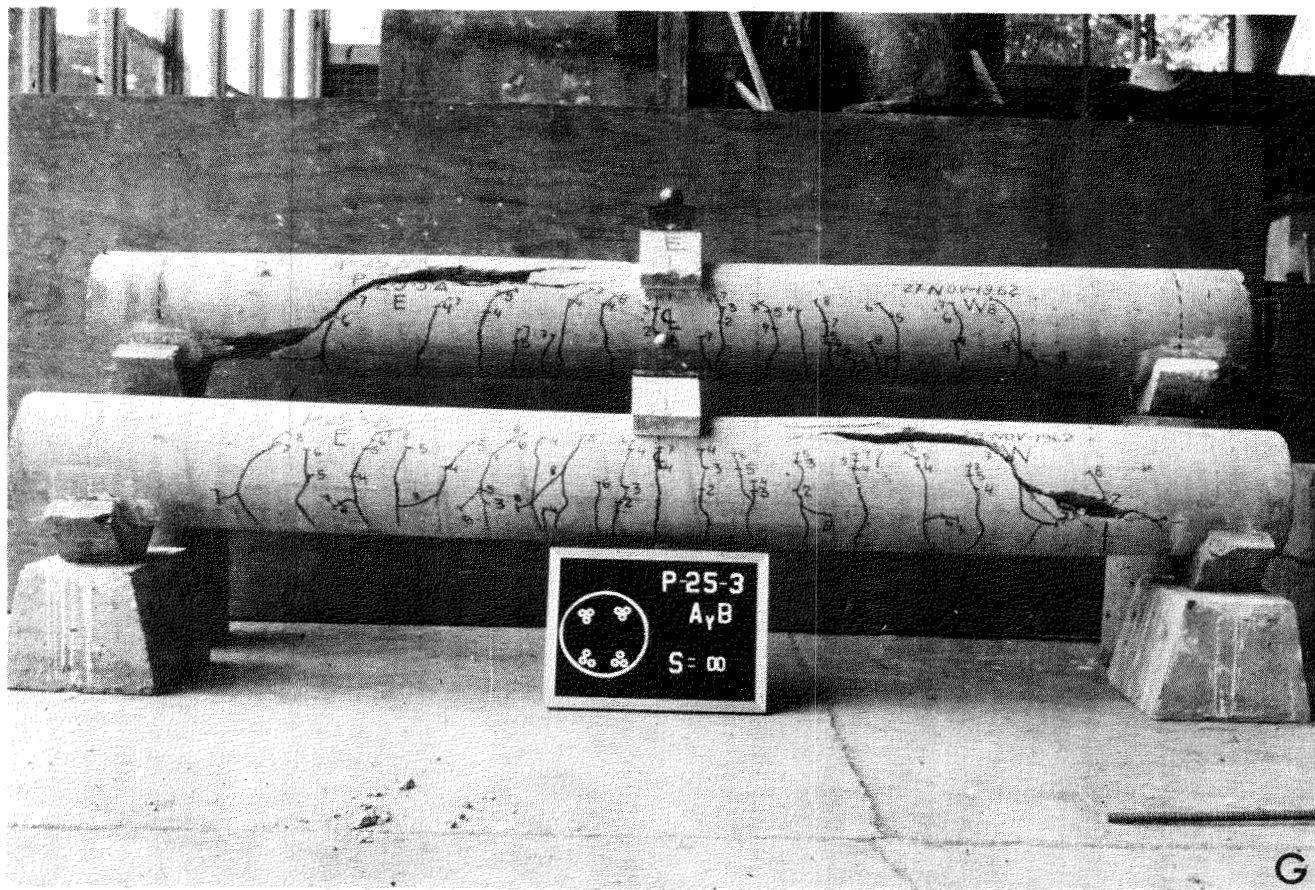


Fig. 9g. Especímenes después de la falla. (continuación)

FIG. 9g PHOTOGRAPHS OF SPECIMENS AFTER FAILURE (continued)

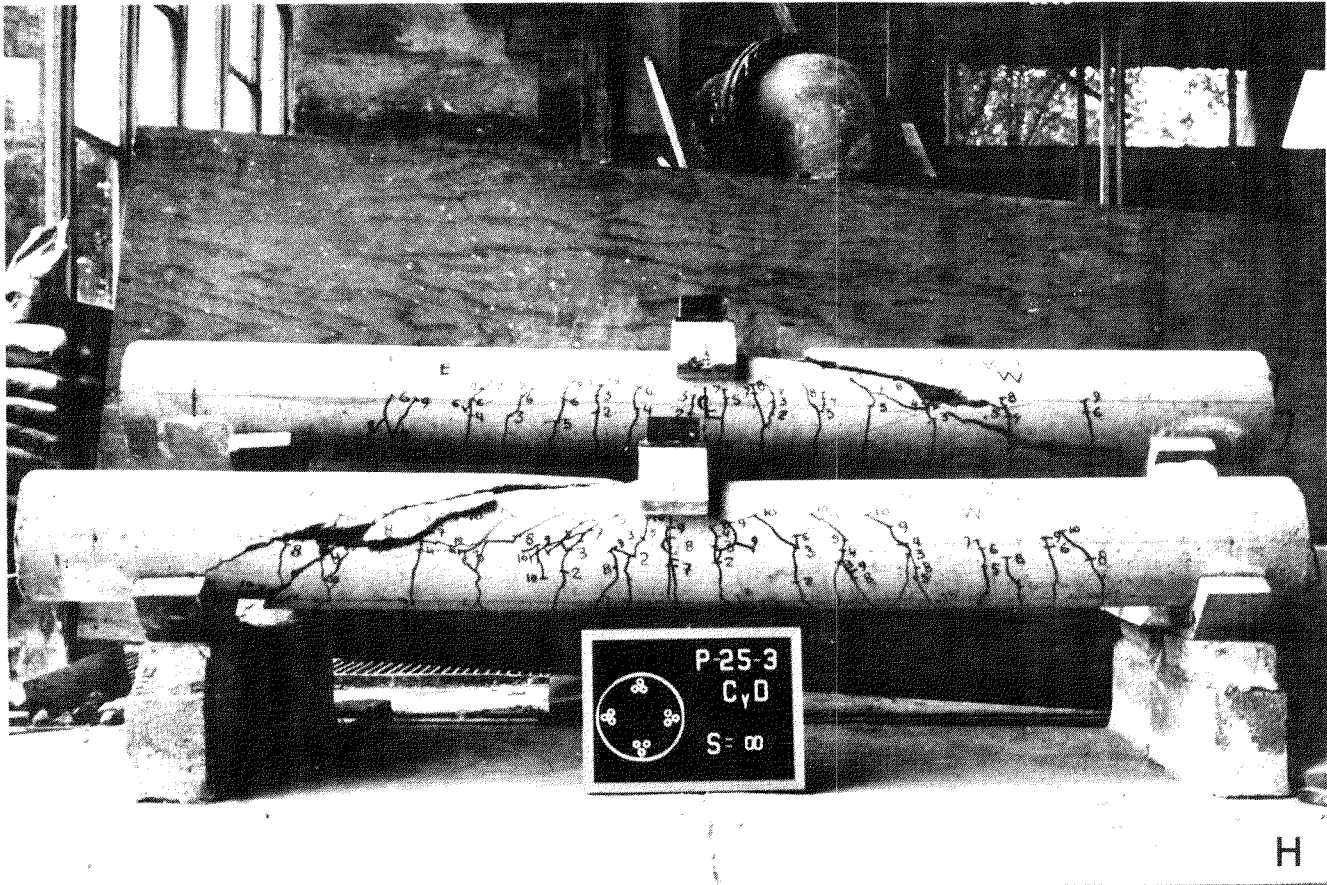


Fig. 9h. Especímenes después de la falla. (continuación)

FIG. 9h PHOTOGRAPHS OF SPECIMENS AFTER FAILURE (continued)

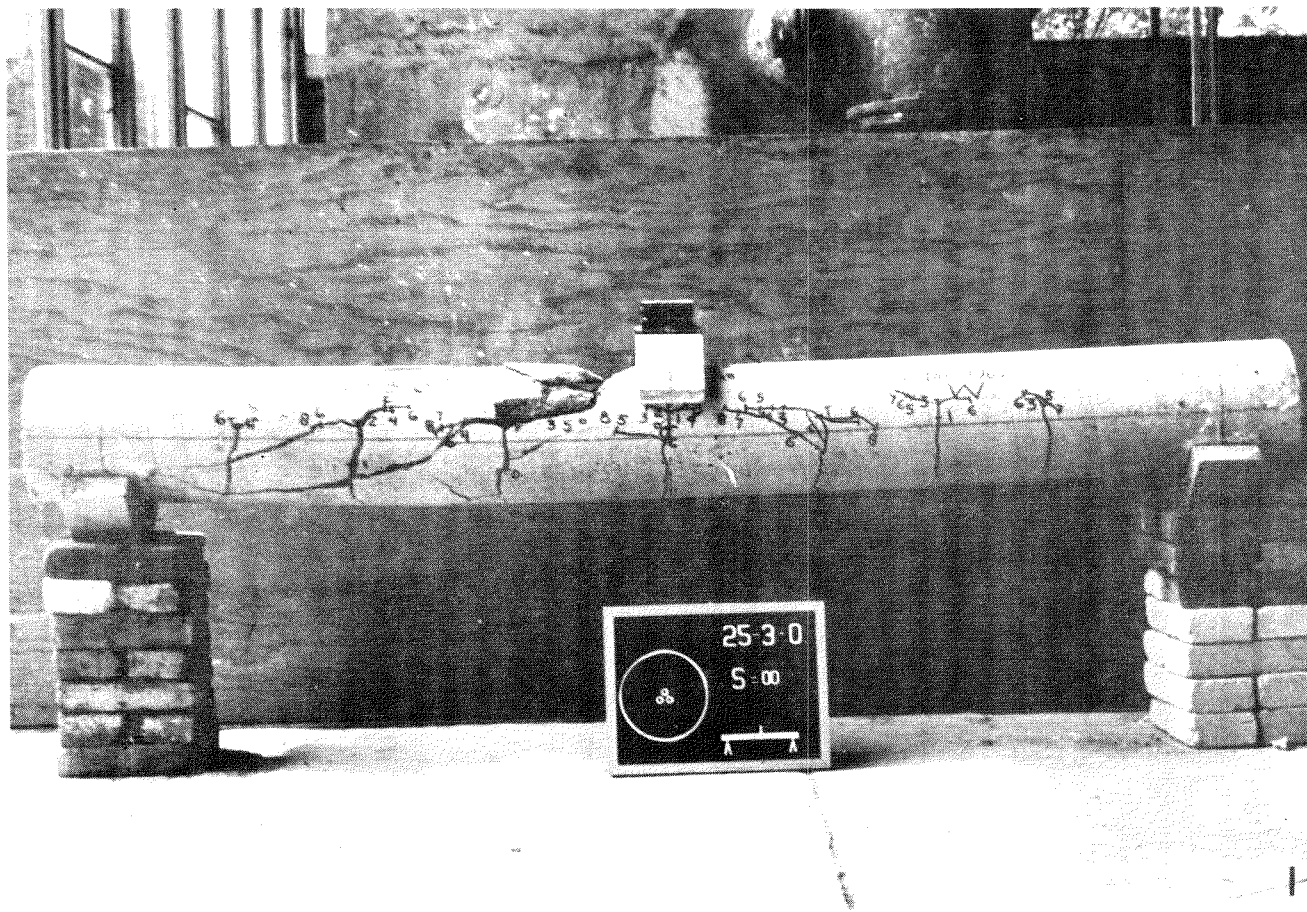


Fig. 9i. Especímenes después de la falla. (continuación)

FIG. 9i PHOTOGRAPHS OF SPECIMENS AFTER FAILURE (continued)

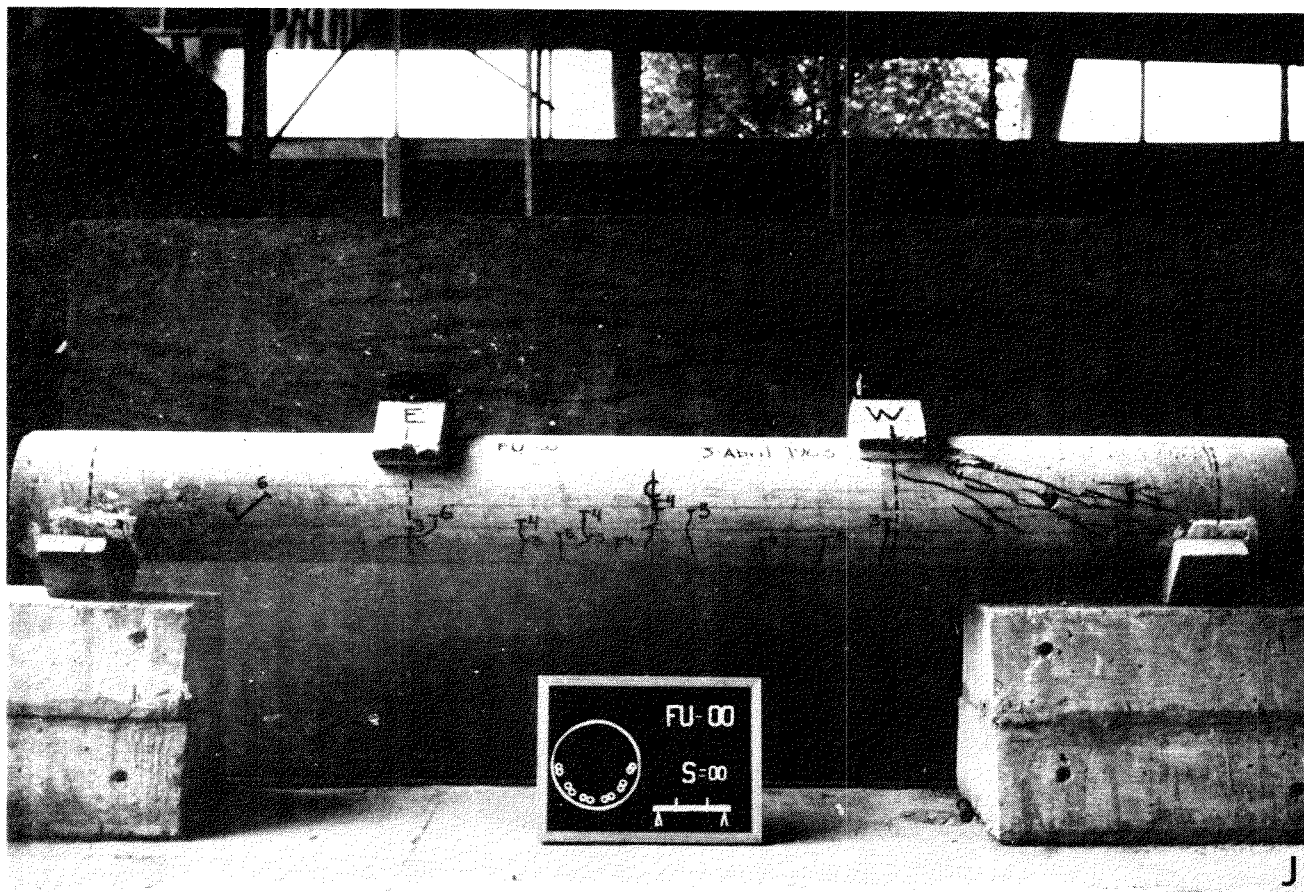


Fig. 9j. Especímenes después de la falla. (continuación)

FIG. 9j PHOTOGRAPHS OF SPECIMENS AFTER FAILURE (continued)

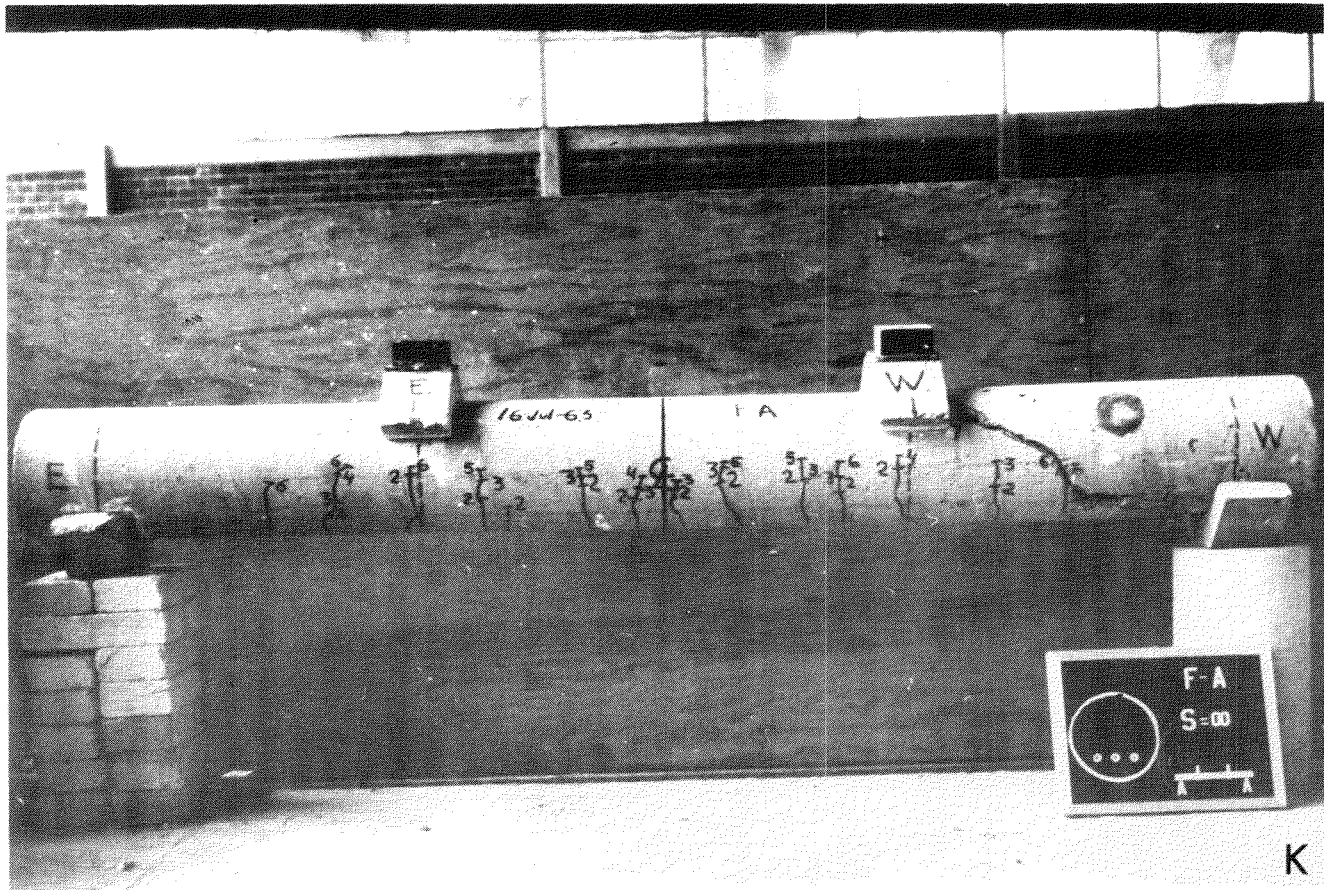


Fig. 9k. Especímenes después de la falla. (continuación)

FIG. 9k PHOTOGRAPHS OF SPECIMENS AFTER FAILURE (continued)

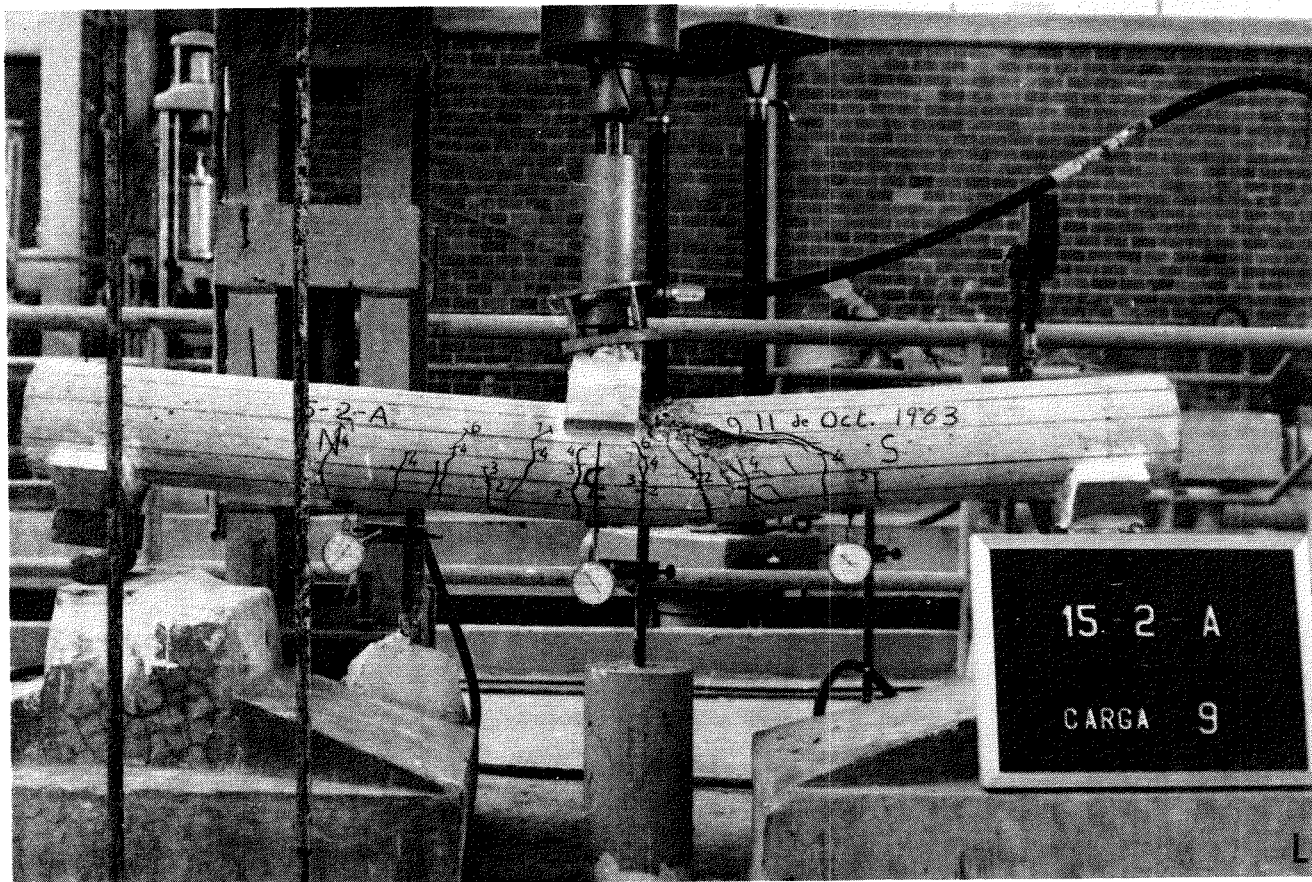


Fig. 91. Especímenes después de la falla. (continuación)

FIG. 91 PHOTOGRAPHS OF SPECIMENS AFTER FAILURE (continued)

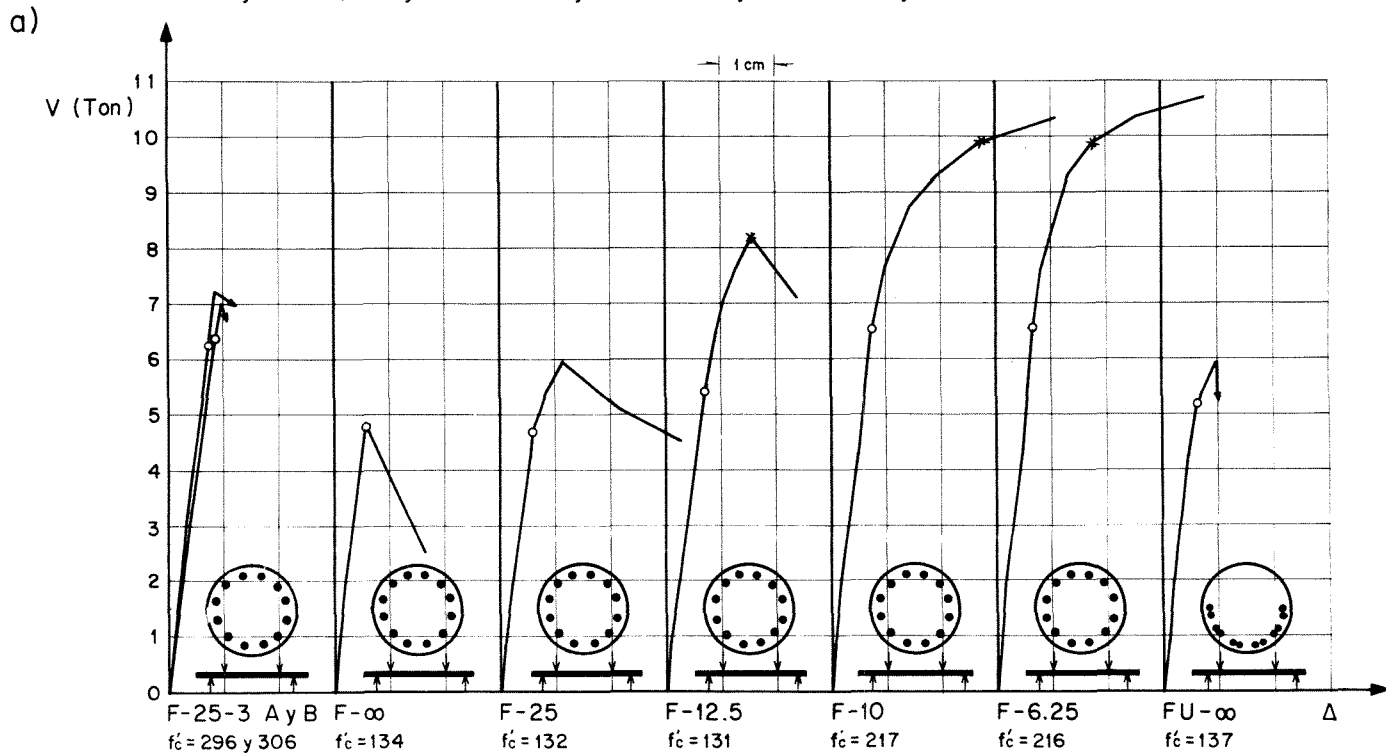
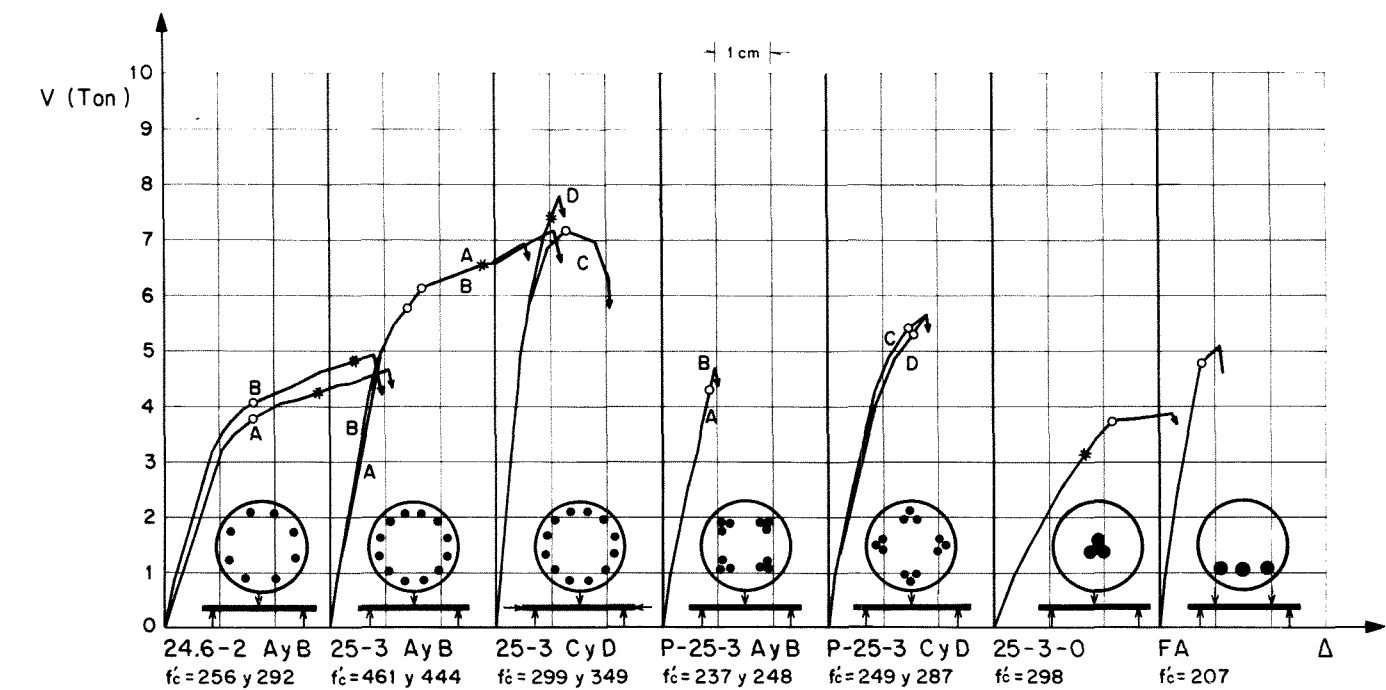


FIG. 10 LOAD-DEFLECTION CURVES

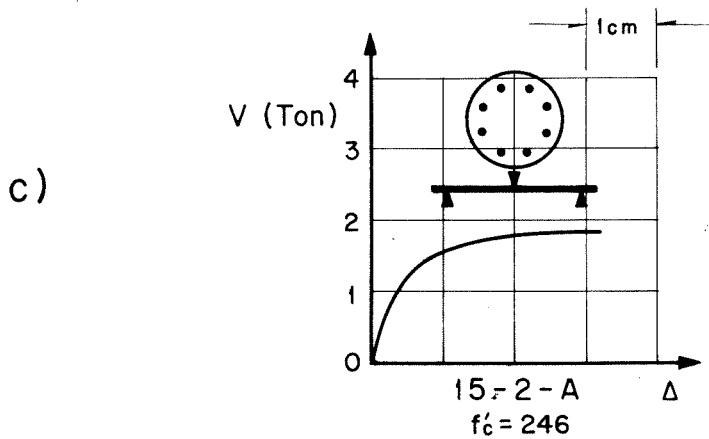
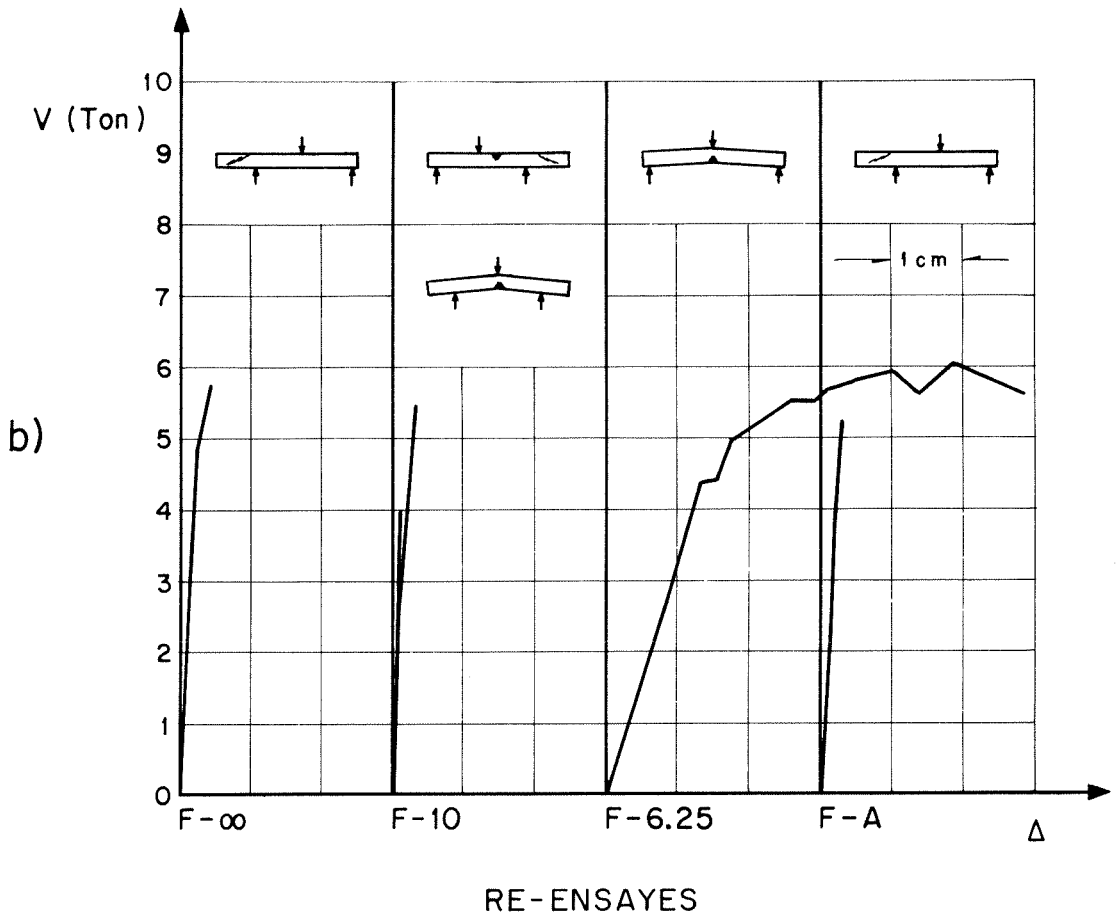
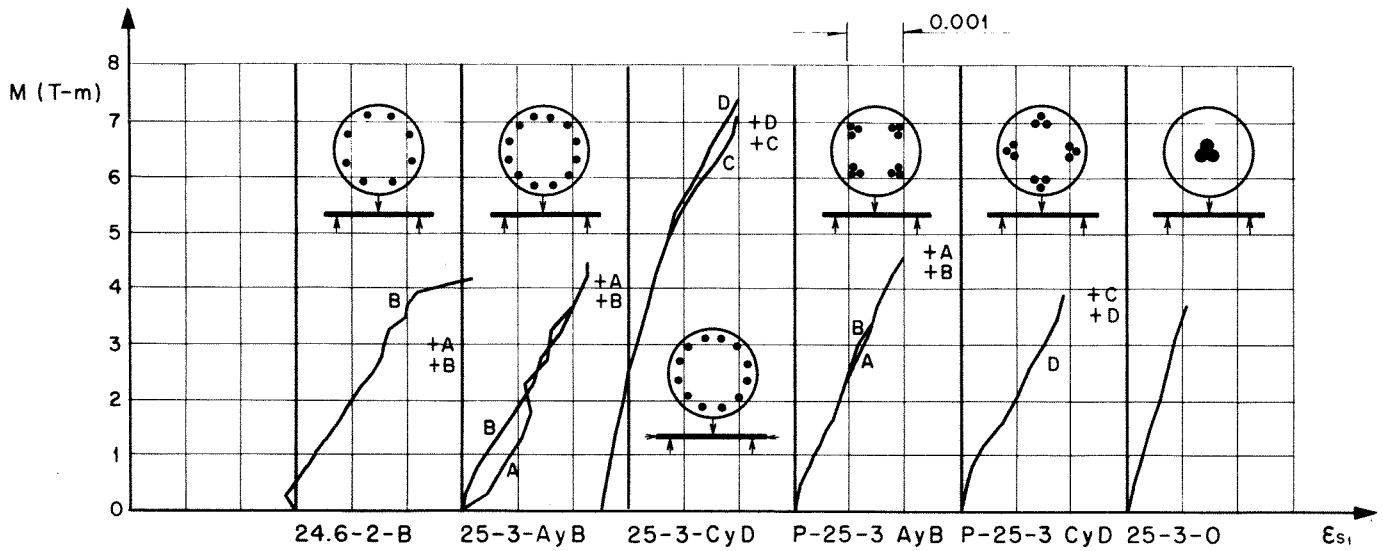


FIG. 10 CURVAS DE CARGA E DEFLEXÃO

FIG. 10 LOAD-DEFLECTION CURVES



+ Valores calculados para la primera fluencia

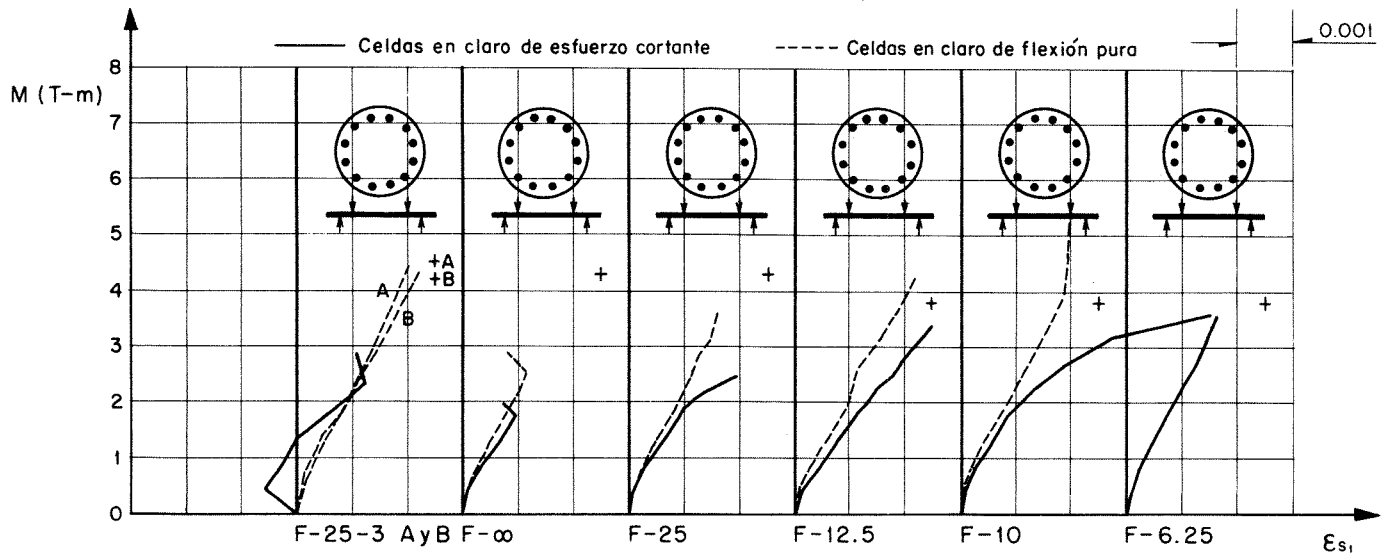


FIG. 11 MOMENT-STRAIN CURVES FOR LOWER LAYER OF STEEL

FIG. 12 TYPICAL SHEAR-STRAIN CURVES FOR LONGITUDINAL STEEL IN SPECIMEN 25-3-C

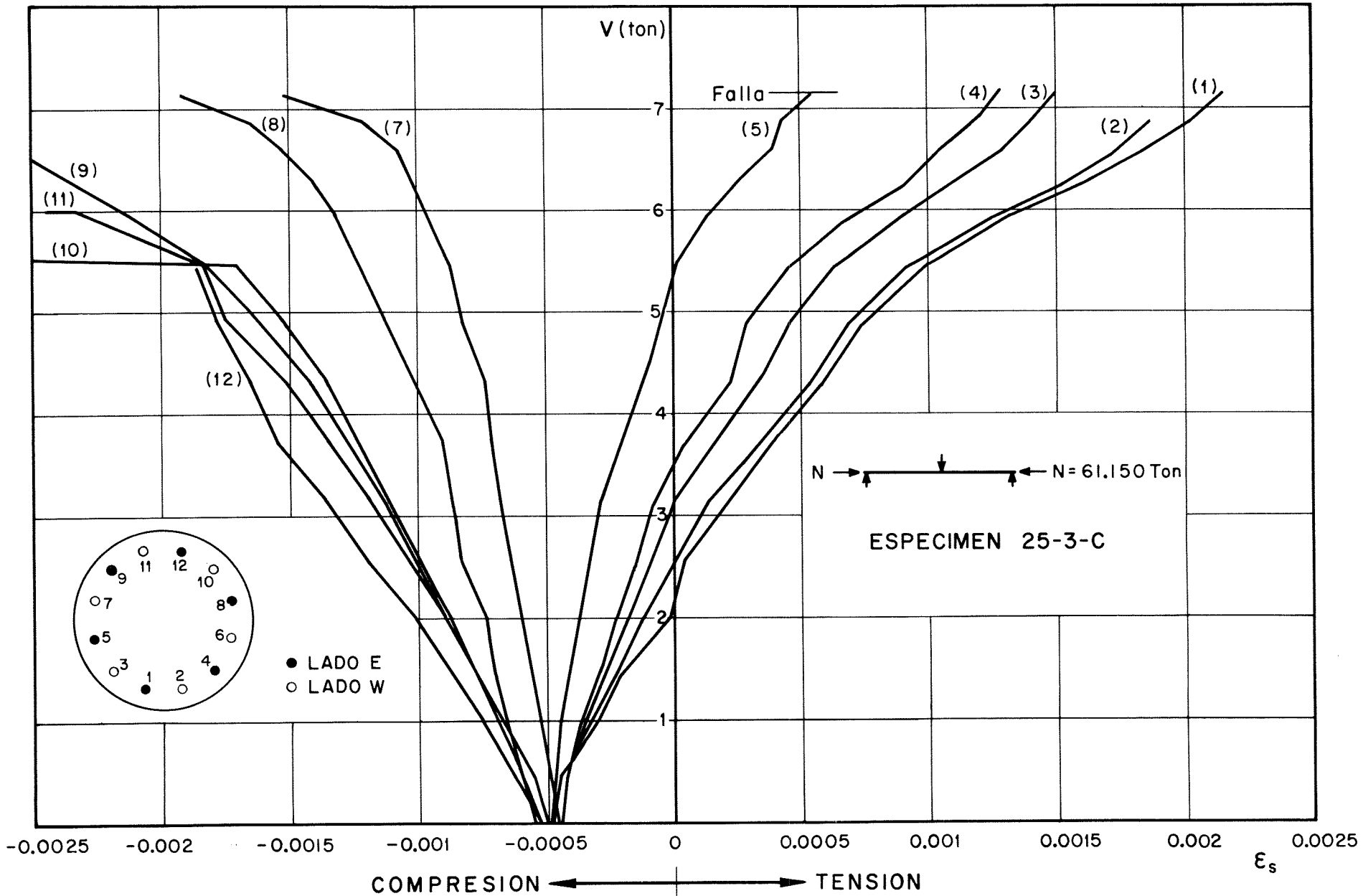


FIG. 13 TYPICAL DISTRIBUTION OF CONCRETE STRAINS

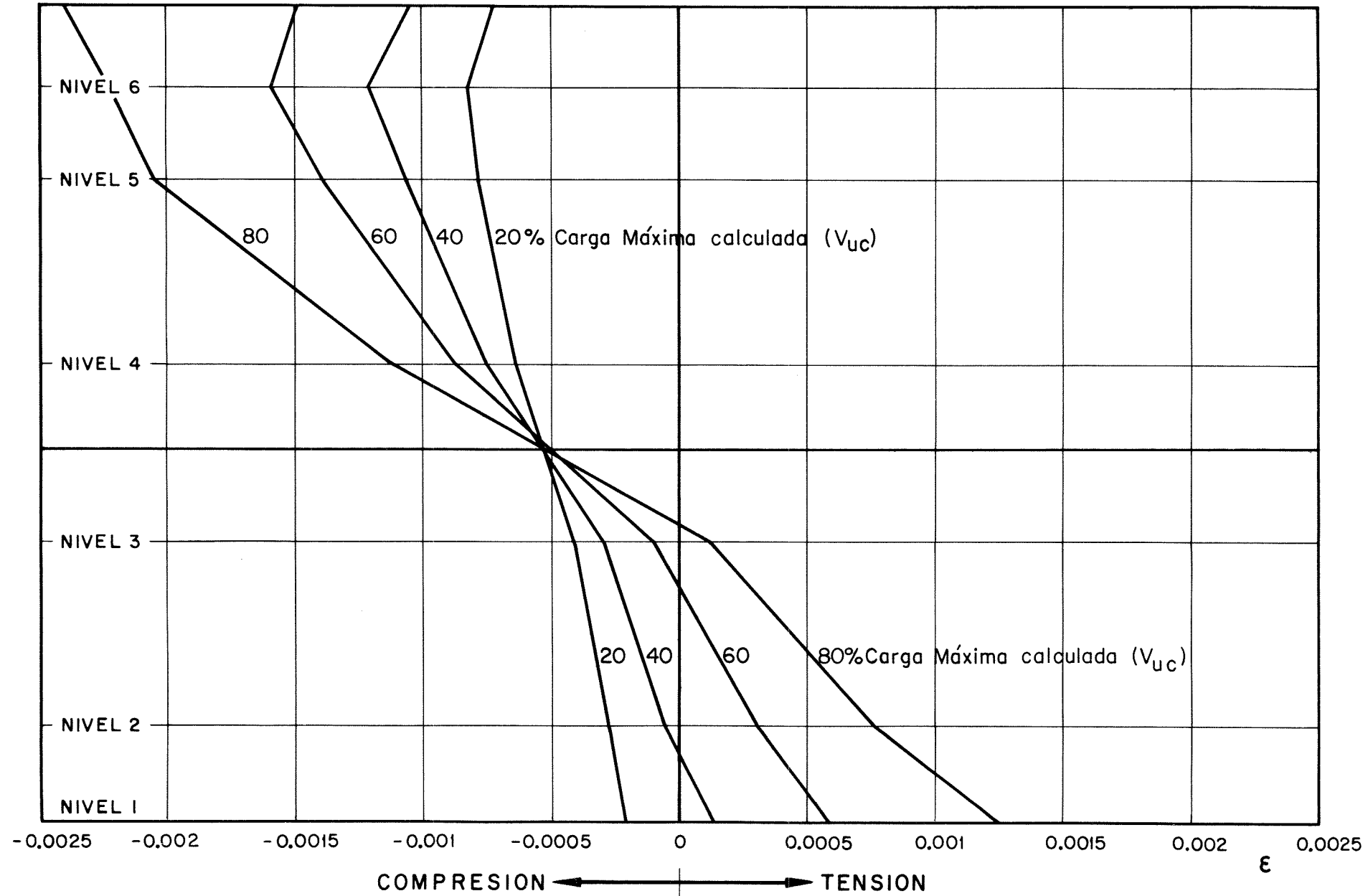


FIG. 14 SHEAR-STRAIN CURVES OF TRANSVERSE STEEL

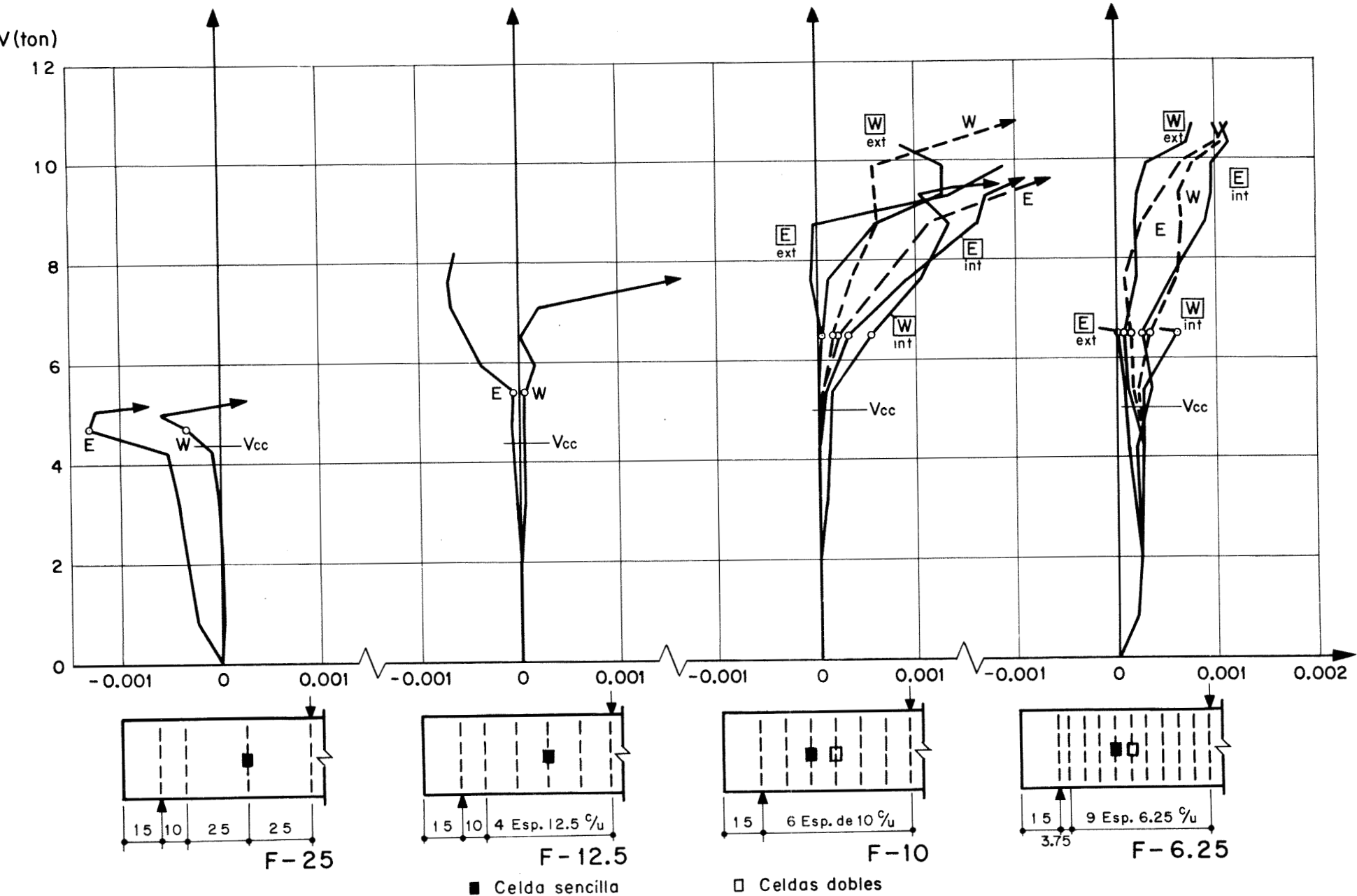


FIG. 15 COMPARISON OF TEST RESULTS WITH THE ACI-ASCE-426 PROPOSED EXPRESSION
 MODIFIED BY THE PARAMETERS OF COMBINATION 14, TABLE 5

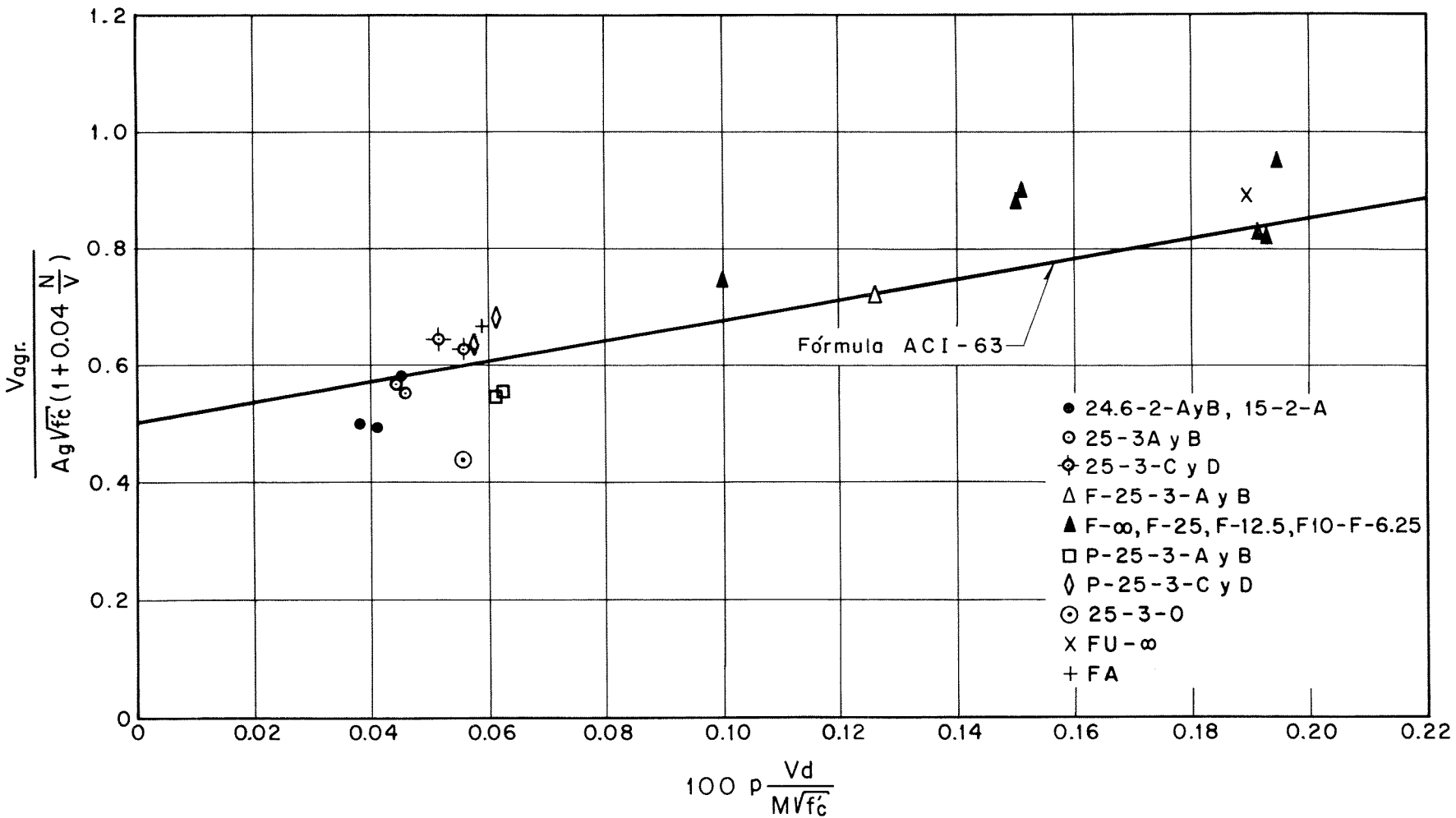


FIG. 15 COMPARISON OF TEST RESULTS WITH THE ACI-ASCE-426 PROPOSED EXPRESSION MODIFIED BY THE PARAMETERS OF COMBINATION 14, TABLE 5